ELECTRO PERSULPHATE OXIDATION OF BIOLOGICALLY TREATED PALM OIL MILL EFFLUENT (POME): POST TREATMENT

CHONG JIA WEI

UNIVERSITI TUNKU ABDUL RAHMAN

ELECTRO PERSULPHATE OXIDATION OF BIOLOGICALLY TREATED PALM OIL MILL EFFLUENT (POME): POST TREATMENT

CHONG JIA WEI

A project report submitted in partial fulfilment of the requirements for the award of Bachelor of Engineering (Hons.) Environmental Engineering

Faculty of Engineering and Green Technology
Universiti Tunku Abdul Rahman

September 2016

DECLARATION

I hereby declare that this project is based on my original work except for citations and quotations which have been duly acknowledged. I also declare that it had not been previously and concurrently submitted for any other degree or award at UTAR or other institutions.

Signature :

Name : Chong Jia Wei

ID No. : 12AGB00364

Date :

APPROVAL OF SUBMISSION

I certify that this project report entitled **"ELECTRO PERSULPHATE OXIDATION OF BIOLOGICALLY TREATED PALM OIL MILL EFFLUENT (POME): POST TREATMENT"** was prepared by **CHONG JIA WEI** has met the required standard for submission in partial fulfilment of the requirements for the award of Bachelor of Engineering (Hons.) Environmental Engineering at Universiti Tunku Abdul Rahman.

Approved by,

Signature :

Supervisor : Dr. Mohammed J.K. Bashir

Date :

ACKNOWLEDGEMENTS

First and foremost, I sincerely thank to my research supervisor, Dr. Mohammed J.K. Bashir who had provided me his professional guidance throughout this period of time. I would also like to thank my moderator, Mr. Wong Ling Yong for his valuable effort and time in evaluating my research.

Besides, I would like to take this opportunity to thank the lab officers for their precious knowledge and techniques during each stage of the experimental work. Next, I am thankful to Tian Siang Oil Mill (Air Kuning) Sdn. Bhd. for allowing me to conduct the on-site sample collection.

Furthermore, I would also like to express my gratitude to my beloved family members for their kind caring and support. Last but not least, I deeply thank to my fellow friends for their unconditional assistance.

ELECTRO PERSULPHATE OXIDATION OF BIOLOGICALLY TREATED PALM OIL MILL EFFLUENT (POME): POST TREATMENT

ABSTRACT

Generation of raw palm oil mill effluent (POME) has rocketed over the past few decades. Due to palm oil is versatile in several applications for either food or non-food uses. Conventional biological treatment is considered as one of the best methods to degrade organics in the POME. However, biologically treated effluent is unable to fulfill regulatory discharge standards decreed by Environmental Quality Act (EQA) 1974 in which post treatment is necessary. Thus, electro persulphate oxidation was introduced as a post treatment to further treat biologically treated POME to achieve stringent discharge standards for the first time. Using response surface methodology (RSM), optimum operational conditions such as current density, contact time, initial pH, and persulphate ($S_2O_8^{2-}$) dosage were empirically determined. Hence, 77.70 % of chemical oxygen demand (COD), 97.96 % of colour, and 99.72 of suspended solids (SS) removal were obtained under 45 mA/cm^2 of current density, 45 min of contact time, pH 4, and 0.892 g of $S_2O_8^{2-}$. Through analysis of variance (ANOVA), determination of coefficients (R^2) were acquired with values of 0.9881, 0.9612, and 0.9589 for each quadratic model of COD, colour, and SS removal. High R^2 values as close to 1 indicate each quadratic model is statistically desirable and has reasonable agreement to experimental data. Upon these findings, electro persulphate oxidation had been proved that it is an effective post treatment due to its promising performance.

TABLE OF CONTENTS

LIST OF TABLES

LIST OF FIGURES

LIST OF SYMBOLS/ABBREVATIONS

AOP	Advanced Oxidation Process
ANOVA	Analysis of Variance
AP	Adequate Precision
BOD	Biological Oxygen Demand
CCD	Central Composite Design
COD	Chemical Oxygen Demand
CPO	Crude Palm Oil
CSTR	Continuous Stirred Tank Reactor
DO	Dissolved Oxygen
DOE	Department of Environmental
DOE	Design-Expert®
EFB	Empty Fruit Bunch
EQA	Environmental Quality Act
Fe^{2+}/H_2O_2	Ambient-Fenton Process
$Fe^{2+}/H_2O_2/UV$	Solar-Fenton Process
FFB	Fresh Fruit Bunch
HUASB	Hybrid Up-Flow Anaerobic Sludge Blanket
ICP-MS	Inductively Coupled Plasma-Mass Spectrophotometer
MBR	Membrane Bioreactor
MF	Microfiltration
OER	Oxygen Evolution Reaction
O&G	Oil and Grease
POME	Palm Oil Mill Effluent
PPF	Palm Pressed Fibre
RSM	Response Surface Methodology
R^2	Determination of Coefficient
SS	Suspended Solids
TS	Total Solids
UASB	Up-Flow Anaerobic Sludge Blanket
UF	Ultrafiltration
UV/H_2O_2	Hydrogen Peroxide Photolysis
VS	Volatile Solids

Al	Aluminium
Al^{3+}	Aluminium Ions
$Al(OH)_3$	Aluminium Hydroxide
CH_4	Methane

CO_2	Carbon Dioxide
Cl_2	Chlorine
ClO^-	Hypochlorite Ions
Cr	Chromium
$Cr_2O_7^{2-}$	Dichromate Ions
DNTs	Dinitrotoluenes
F_2	Fluorine
Fe	Iron
Fe^{2+}	Ferrous Ions
Fe^{3+}	Ferric Ions
$Fe(OH)_3$	Ferric Hydroxides
H^+	Hydrogen Ions
H_2	Hydrogen Gas
H_2O	Water
H_2O_2	Hydrogen Peroxide
$HOPhX^{\cdot}$	Organics Free Radicals
HNO_3	Nitric Acid
M^{n+}	Metal Ions
MO_x	Metal Oxide
$MO_x(\,)$	Surface Sites
$M(OH)_n$	Metal Hydroxides
$MO_x(\cdot OH)$	Adsorbed Hydroxyl Radicals
MO_{x+1}	Higher Oxides
$Na_2S_2O_8$	Sodium Persulphate
$NH_3 - N$	Ammoniacal Nitrogen
Ni	Nickel
$O^{\cdot -}$	Oxide Radicals
O_2	Oxygen
O_3	Ozone
$\cdot OH$	Hydroxyl Radicals
OH^-	Hydroxyl Ions
Pb	Lead
PbO_2	Lead Oxide
$R^{\cdot}$	Organics Free Radicals
$RO_2^{\cdot}$	Peroxy Radicals
$ROOH$	Organic Hydrogen Peroxides
$SO_4^{\cdot -}$	Sulphate Radicals
$S_2O_8^{2-}$	Persulphate
$SnO_2 - Sb_2O_5$	Antimony-Doped Tin Oxide
Zn	Zinc

atm	Atmospheric Pressure
℃	Degree Celcius
cm	Centimetre
cm^2	Centimetre Square
g	Gram
K	Kelvin
mA/cm^2	Milliampere per Centimetre Square
min	Minute(s)

mg/L	Miligram per Litre
ml	Mililitre
NTU	Nephelometric Turbidity Unit
ppb	Parts per Billion
$PtCo$	Platinum Cobalt
rpm	Round per Minute

LIST OF APPENDICES

CHAPTER 1

INTRODUCTION

1.1 Background of Study

Currently, Malaysia is the second largest palm oil producer and exporter in the world that indicates palm oil industry plays a significant role in the country's economy (Abdullah and Sulaiman, 2013; Gan and Li, 2014; MPOB, 2011). The unique composition of palm oil allows it versatile in different applications, including food manufacturing, chemical, cosmetic, and pharmaceutical industries (Azoddein, Haris and Azli, 2015). From 1960 to 2014, land areas planted with oil palm increased from 0.05 to 5.39 *million hectares* which represented a phenomenal growth as shown in Figure 1.1.

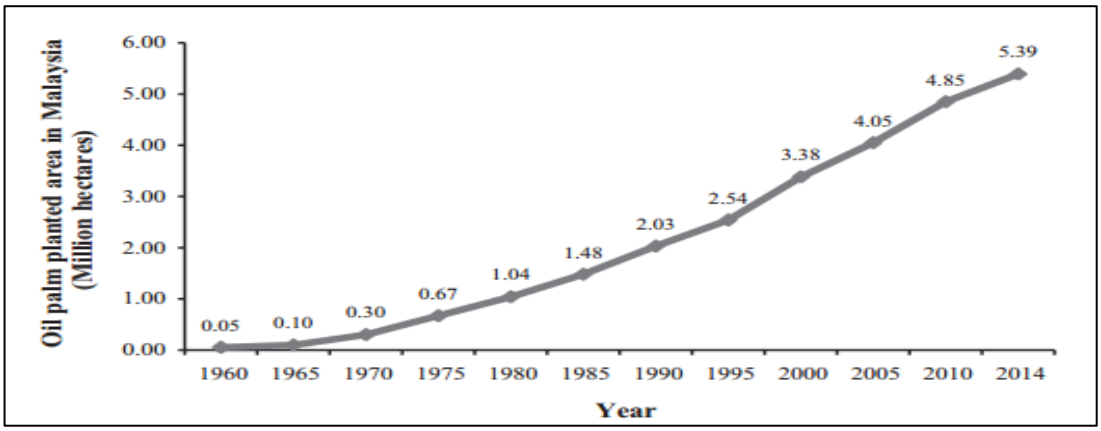

Figure 1.1 Expansion of Oil Palm Planted Area in Malaysia from 1960 to 2014 (Awalludin et al., 2015)

Escalation of planted hectares resulted in formation of large quantities of polluted wastewater and referred as palm oil mill effluent (POME). Generally, production of palm oil can be differentiated into dry and wet process, where the wet process is considered as the most ordinary method used in Malaysia (Ujang, Salmiati and Salim, 2010). By applying the wet process, POME is a combination of liquid wastes from sterilization, clarification as well as hydrocyclone separation (Badroldin, 2010; Hassan, Kee and Al-Kayiem, 2013). This is because large quantities of water (H_2O) are utilized for extraction of crude palm oil (CPO) from fresh fruit bunch (FFB), where over 50 % of H_2O ends up as POME (Badroldin, 2010; Ujang, Salmiati and Salim, 2010). If 1 $tonne$ of CPO is yielded, about 3.5 m^3 or 2.5 $tonnes$ of POME are produced (Madaki and Seng, 2013).

Tremendous increased of production of CPO have always been a threat to the environment. Direct discharging of raw or partially treated POME with high content of organics and nutrients into nearby watercourses can lead to environmental pollutions (Hassan, Kee and Al-Kayiem, 2013). Oxygen depletion is one of the pollutions that occurs in natural waterway and ends up with suffocation of aquatic organisms (Badroldin, 2010; Jones-Lee and Lee, 2005; Madaki and Seng, 2013). On top of that, human health is also affected especially those who lives at downstream areas (Madaki and Seng, 2013). Furthermore, POME releases odour to the environment, and reduces air quality as well (Abdullah and Sulaiman, 2013). Thus, effective treatments should be experimented and introduced in order to conserve the environment in terms of H_2O and air quality.

Biological treatments are mostly and effectively used by palm oil mills for treating raw POME, such as anaerobic, facultative, and aerobic (Abdurahman, Azhari and Rosli, 2013; Aris et al., 2008). However, discharge limits decreed by Environmental Quality Act (EQA) are not always fulfilled after the biological treatments. This is very much due to non-biodegradable or hardly biodegradable organics that still result in high biological oxygen demand (BOD), chemical oxygen demand (COD) as well as suspended Solids (SS). Hence, physico-chemical treatment is recommended as post-treatment for further polishing biologically treated POME to meet the desirable discharge standards. Several post-treatments are well-known in treating biologically treated POME, such as membrane-bioreactor (MBR), adsorption,

ultrasonic irradiation, and advanced oxidation process (AOP). AOP is widely applied by adopting highly reactive hydroxyl radicals ($\cdot OH$) in which unselectively react and oxidize recalcitrant organics into carbon dioxide (CO_2) and H_2O, less harmful or biodegradable substances via hydrogen abstraction and radical addition (Abdullah, 2008; Ameta et al., 2012; Chong et al., 2012; Kommineni et al., 2008; Quiroz et al., 2011; Stasinakis, 2008). $\cdot OH$ are one of the most powerful oxidants with oxidation potential of 2.80 V (Barrera-Díaz et al., 2014). There are several types of AOP used in treating biologically treated POME, such as hydrogen peroxide photolysis (H_2O_2/UV), ambient-Fenton process (Fe^{3+}/H_2O_2), and solar-Fenton process ($Fe^{3+}/H_2O_2/UV$).

Electrooxidation is an AOP that provides high removal efficiency, ease in operation, robustness in configuration, as well as low temperature requirement (Morsi, Al-Sarawy and El-Dein, 2011; Wang, et al., 2012). It is an effective process in organics degradation by using anodic adsorbed oxidants or electrochemically generated oxidants in bulk solution to simultaneously carry out direct and indirect oxidation (Barrera-Díaz et al., 2014; Britto-Costa and Ruotolo, 2012). Performance of the electrooxidation can be enhanced by synergistic effect of oxidants. Different types of oxidants are suitable to be adopted that involve hydrogen peroxide (H_2O_2) and ozone (O_3) with oxidation potential of 1.80 V and 2.10 V (Abdullah, 2008). Furthermore, persulphate ($S_2O_8^{2-}$) are also strong oxidants with oxidation potentials of 2.01 V and originally produced from sodium persulphate ($Na_2S_2O_8$) (Ocampo, 2009; Padmanabhan, 2008). Normally, $S_2O_8^{2-}$ have slow kinetic rate to react with organics, but electrolytic activation is able to generate another strong radicals, known as sulphate radicals ($SO_4^{\cdot-}$) with oxidation potential of 2.60 V (Chung et al., 2012; Ocampo, 2009; Padmanabhan, 2008; Wilson et al., 2013). Since the oxidation potential of $SO_4^{\cdot-}$ is higher than $S_2O_8^{2-}$, so $SO_4^{\cdot-}$ are highly active to induce other species to lose electrons through oxidation which indicates organics degradation is initiated (Szymczycha and Pempkowiak, 2016). Besides, radical inter-conversion is initiated by $SO_4^{\cdot-}$ to generate $\cdot OH$ in the solution (Padmanabhan, 2008). Meanwhile, H_2O_2 is produced via hydrolysis of $S_2O_8^{2-}$ under acidic condition, and subsequently form $\cdot OH$ via cathodic reduction (Barrera-Díaz et al., 2014; Chung et al., 2012).

Therefore, all potential oxidants function simultaneously are capable to perform an effective organics degradation.

On the other hand, electrocoagulation and electrofloatation are initiated in the bulk solution due to required anode and cathode in the electrooxidation. Electrocoagulation is induced by anodic dissolution that generates metal ions (M^{n+}) to destabilise pollutants, and subsequently form loose aggregates (Ni'am et al, 2007; Rahmalan, 2009). Besides that, M^{n+} also react with hydroxyl ions (OH^-) produced at cathode, and form metal hydroxides ($M(OH)_n$). Generally, $M(OH)_n$ have high adsorptive properties which can bond with destabilised pollutants, and form large lattice structures or flocs (Kabdaşlı et al., 2012). These flocs can be removed either via sedimentation or floatation. Formation of hydrogen gas (H_2) bubbles triggered by cathodic reduction of hydrogen ions (H^+) is the main process of electrofloatation. Normally, small H_2 bubbles provide large surface area to attach trapped pollutants or large flocs, and subsequently float to the top surface (Mickova, 2015). In other words, both processes function together with electrooxidation in removing organics, SS as well as heavy metals in the bulk solution.

1.2 Problem Statements

In 2015, Malaysia's CPO production had been increased to 19.96 $million\ tonnes$ (MPOB, 2015) which resulted in excessive of raw POME that must be treated to achieve discharge limits set by EQA 1974. Generally, biological degradation processes are widely and effectively used in treating raw POME, such as anaerobic, facultative and aerobic ponding systems. Malaysia had more than 85 % of palm oil mills used ponding systems because of low capital and operating costs (Abdurahman, Azhari and Rosli, 2013; Bala, Lalung and Ismail, 2014; Madaki and Seng, 2013). Nonetheless, ponding systems require long retention time and large treatment area which consider as limitations (Abdurahman, Azhari and Rosli, 2013; Bala, Lalung and Ismail, 2014; Rupani et al., 2010). Furthermore, failure of achieving discharge standards is encountered after biological treatments because of organics with simple structures are easily degraded, but non-biodegradable organics are very slow

metabolized and degraded (Zheng et al., 2013). Hence, high COD and BOD effluent are discharged into nearby water body that lead to adverse impacts to aquatic life and human health (Fadzil, Zainal and Abdullah, 2013). Also, unaesthetic view is induced by dark brown effluent because of presence of hardly biodegradable lignin and other phenolic compounds after the biological treatments (Mohammed and Chong, 2014; Gomathi et al., 2012).

Researchers had put in effort to investigate an efficient treatment for further polishing biologically treated POME. In this study, electro persulphate oxidation as post-treatment was carried out for the first time. It is a treatment with effects of combination processes, including electrooxidation, electrocoagulation, and electrofloatation. This combination is able to provide high removal efficiency due to synergistic effect of strong oxidants formation, such as $S_2O_8^{2-}$, H_2O_2, $SO_4^{\cdot-}$, and $\cdot OH$ that react and oxidize organics into CO_2 and H_2O, or less harmful or biodegradable substances. Besides, SS, organics, and heavy metals removal rely on M^{n+} and high adsorptive properties of $M(OH)_n$ via anodic dissolution to coagulate pollutants. On top of that, formation of H_2 bubbles from cathodic hydrogen evolution also assists in removal of large flocs by floatation. Thus, several operational conditions have to be considered and analysed in order to achieve better performance, such as electrode, current density, contact time, initial pH as well as $S_2O_8^{2-}$ dosage.

1.3 Study Objectives

This study is conducted for the following objectives:

i. To determine efficiency of electro persulphate oxidation of biologically treated POME.
ii. To investigate effects of current density, contact time, initial pH, and $S_2O_8^{2-}$ dosage on the performance of electro persulphate oxidation.
iii. To evaluate optimum performance of electro persulphate oxidation by using response surface methodology (RSM).

CHAPTER 2

LITERATURE REVIEW

2.1 Palm Oil Industry in Malaysia

Malaysia is currently the second largest palm oil producer and exporter in the world after being overtaken by Indonesia in 2008 (Abdullah and Sulaiman, 2013; Gan and Li, 2014; MPOB, 2011). From 2008 to 2015, production of CPO in Malaysia raised from 17.73 to 19.96 *million tonnes* as shown in Table 2.1 (MPOB, 2008; MPOB, 2015). From 2008 to 2015, export of palm oil in Malaysia increased from 15.41 to 17.45 *million tonnes* as shown in Table 2.2 (MPOB, 2008; MPOB, 2015). Both phenomena proved that palm oil demand had received worldwide attention. This is because palm oil is versatile in several applications, such as food manufacturing, chemical, cosmetic, and pharmaceutical industries (Azoddein, Haris and Azli, 2015). Palm oil product such as vegetable oil receives significant demand because of growth in global population (Mahat, 2012). About 28 % of vegetable oil was traded globally in 2011 (Gan and Li, 2014). Vegetable oil derived from palm oil is free of death-inducing cholesterol, trans-fatty acid, and rich in Vitamin A and E that is good in minimising heart and eyes diseases. For non-food use, palm oil by-product acts as feedstock to replace petrochemical (Oleo-chemical) to manufacture soap, cosmetic and cleaning product (MPOC, 2006). Therefore, highly global palm oil demand has resulted in economic growth in Malaysia.

Table 2.1 Malaysia's Production of CPO from 2008 to 2015 (MPOB, 2008; MPOB, 2015)

Year	Total CPO Production, $million\ tonnes$
2008	17.73
2015	19.96

Table 2.2 Malaysia's Export of Palm Oil from 2008 to 2015 (MPOB, 2008; MPOB, 2015)

Year	Total Export of Palm Oil, $million\ tonnes$
2008	15.41
2015	17.45

Total landmass in Malaysia is 32.86 $million\ hectares$, a variety of food and economic crops occupy around 20 % or 6.570 $million\ hectares$ out of total landmass, including oil palm, rubber, cocoa, coconut and others (MPOC, 2006). Oil palm plantation occupies about 4.170 $million\ hectares$ out of 5.556 $million\ hectares$ of land used for selected tree crops as shown in Figure 2.1. It serves as closed green canopy to protect the environment via a natural process called photosynthesis (Miettinen et al., 2012; MPOC, 2006). CO_2 is one of the greenhouse gases that traps heat and increases atmospheric temperature, eventually results in global warming. Oil palm is capable to absorb large amount of CO_2 and release more oxygen (O_2) as compared to soy bean. Oil palm absorbed 270.70 $million\ tonnes$ of CO_2 from, and returned 196.80 $million\ tonnes$ of O_2 to the atmosphere from a mere 9.24 $million\ hectares$ of total global planted area. On the other hand, soy bean absorbed 325.20 $million\ tonnes$ of CO_2 from, and returned 236.50 $million\ tonnes$ of O_2 to the atmosphere from a huge area of 92.40 $million\ hectares$ of total global planted area (MPOC, 2006). Table 2.3 shows the performance between oil palm and soybean in CO_2 sequestration. From the comparison, oil palm proved an excellent

ability in absorption of CO_2, and releasing of O_2 in order to reduce effects of greenhouse gases.

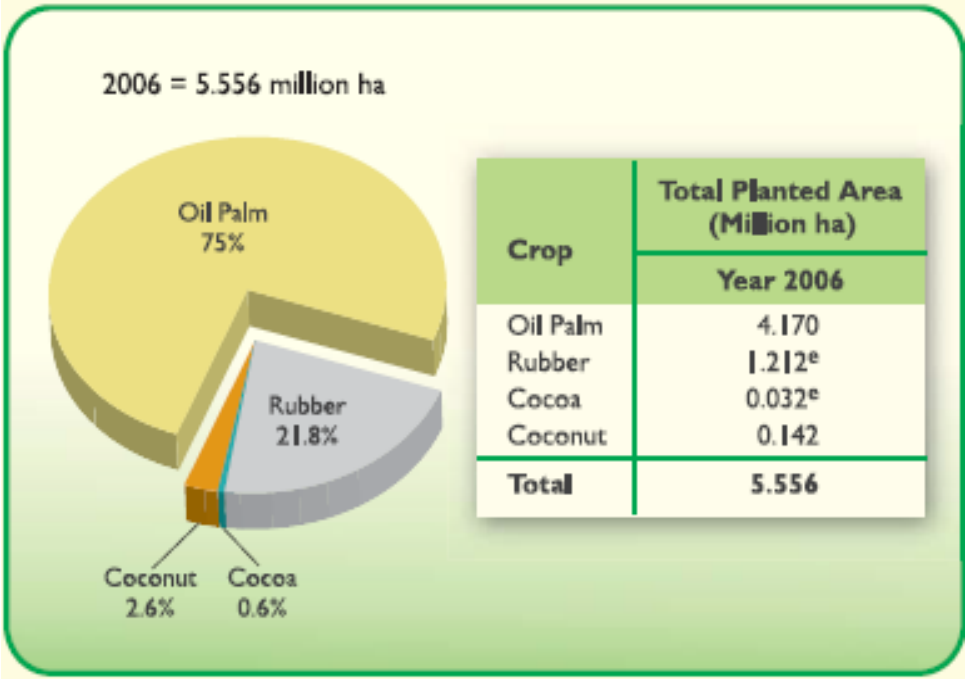

Figure 2.1 Land Used of Selected Tree Crops in Malaysia (MPOC, 2006)

Table 2.3 Performance between Oil Palm and Soybean in CO_2 Sequestration (MPOC, 2006)

Oil Crop	Total Global Planted Area, *million hectares*	O_2 Released, *million tonnes*	CO_2 Absorbed, *million tonnes*	Average O_2 Released, *tonne per hectare*	Average CO_2 Absorbed, *tonne per hectare*
Oil Palm	9.24	196.80	270.70	21.30	29.30
Soybean	92.40	236.50	325.20	2.56	3.52

Furthermore, palm oil is used as raw material in biodiesel production or fuel to be burnt in power station for electricity generation (Calabria and Capata, 2012; Nagi, Ahmed and Nagi, 2008). From 2006 to 2013, Malaysia had exported 900

$thousand\ tons$ of biodiesel derived from palm oil, mainly to Europe and United States (Gan and Li, 2014). Palm biodiesel is an alternative fuel that acquires high fossil energy balance, and with that it is able to overcome issues of increasing price and limited reserve of fossil fuels. Besides, burning of palm biodiesel does not contribute increase of CO_2 in the atmosphere as it only releases CO_2 absorbed earlier through photosynthesis, and is considered as carbon neutral (MPOC, 2007; Nagi, Ahmed and Nagi, 2008). On top of that, it is enriched with oxygen content that improves combustion efficiency in order to minimise formation of carbon monoxide (CO) through incomplete combustion. Sulphur-free is another benefit offered by palm biodiesel to reduce sulphur oxide (SO_x) emissions that result in acid rain formation (Nagi, Ahmed and Nagi, 2008).

2.2 Wastes Generation from Palm Oil Industry

Different wastes in large quantities are generated after extraction of CPO, including empty fruit bunch (EFB), palm pressed fibre (PPF), shell as well as POME (Abdullah and Sulaiman, 2013). Table 2.4 shows the percentage of product or waste generated per bunch of fresh fruit. Furthermore, extraction of CPO from FFB requires large quantities of water, where over 50 % of water ends up as POME (Badroldin, 2010; Ujang, Salmiati and Salim, 2010). If 1 $tonne$ of CPO is yielded, about 3.5 m^3 or 2.5 $tonnes$ of POME are produced. In order to meet both domestic and global demand of palm oil products, considerable production and processing of palm oil lead to increase of POME generation (Madaki and Seng, 2013).

Table 2.4 Percentage by Weight of Product or Waste Generated per Bunch of Fresh Fruit (Abdullah and Sulaiman, 2013)

Product or Waste	**Percentage by Weight,** %
Palm Oil	21
Palm Kernel	7
Shell	6
PPF	15
EBF	23
POME	28

2.3 Characteristics of Raw POME

POME is an agro-industrial waste that is generated in large quantities from a series of processes of CPO extraction. It is a combination of wastewater generated and discharged from sterilization of FFB, clarification of extracted CPO as well as hydrocyclone separation of kernel in which large quantities of hot water and steam are utilized (Badroldin, 2010; Hassan, Kee and Al-Kayiem, 2013). Table 2.5 shows the percentage of POME produced from the sterilization, clarification, and hydrocyclone separation.

Table 2.5 Percentage of POME Produced from Sterilization, Clarification, and Hydrocyclone Separation (Badroldin, 2010)

Processing Operation	**Percentage of POME,** %
Sterilization	36
Clarification	60
Hydrocyclone Separation	4

Physical characteristics of raw POME are dark brownish and viscous. Generally, it is hot at temperature of 80 - 90 ℃ because of sterilization (Bala, Lalung

and Ismail, 2014). Formation of organic acid in fermentation process leads to raw POME with pH 4 - 5 (Rupani et al., 2010). It exists in form of colloidal slurry of H_2O, oil, and fine cellulolytic wastes in which made up of 95 - 96 % of H_2O, 0.6 - 0.7 % of oil, and 4 - 5 % of total solids (TS) including 2 - 4 % of SS (Badrolin, 2010; Hassan, Kee and Al-Kayiem, 2013). SS are organic matters mainly derived from cellulolytic debris of fruits known as palm mesocarp, and about 50 % of POME is constituted by SS. It is also a non-toxic liquid waste as no additional of chemicals in CPO extraction (Bala, Lalung and Ismail, 2014). Generally, raw POME has high content of organics and solids, where its composition varies from different batches, processing techniques as well as age or type of fruits (Madaki and Seng, 2013). Table 2.6 shows the typical characteristics of raw POME produced from palm oil mills.

Table 2.6 Typical Characteristics of Raw POME (Madaki and Seng, 2013; MPOB, 2014)

*Parameter	Mean	Range
pH	4.2	3.4 - 5.2
Temperature	-	80 - 90
BOD	25,000	10,250 - 43,750
COD	51,000	15,000 -100,000
TS	40,000	11,500 - 79,000
SS	18,000	5,000 - 54,000
Volatile Solids (VS)	34,000	9,000 - 72,000
Oil and Grease (O&G)	6,000	130 - 18,000
Ammoniacal Nitrogen ($NH_3 - N$)	35	4 - 80
Total Nitrogen	750	180 - 1,400

*All parameters are expressed in mg/L, except pH and temperature (℃).

2.4 Regulatory Discharge Standards of POME

A licensing system had been implemented by Malaysia government to reduce environmental issues through effluent standards and effluent charges (Igwe and Onyegbado, 2007). Regulatory control over discharge of POME was established through Environmental Quality (Prescribed Premises) (Crude Palm Oil) Regulations, 1977 issued under the EQA 1974 and strictly enforced by the Department of Environmental (DOE). Hence, all palm oil mills are claimed to follow the prescribed rules to discharge POME into watercourses. Furthermore, discharging limit of BOD had been tightened by DOE from 100 mg/L reduced to 20 mg/L for palm oil mills in certain environmentally sensitive areas in Sabah and Sarawak (Ravindra, 2015). Table 2.7 shows the regulatory discharge standards of POME according to EQA 1974.

Table 2.7 Regulatory Discharge Standards of POME According to EQA 1974 (Lorestani, 2006; Shahrifun, et al., 2015)

*Parameters	Regulatory Discharge Standards
pH	5 - 9
Temperature	45
BOD	100
COD	1,000
TS	1,500
SS	400
VS	-
O&G	50
$NH_3 - N$	150
Total Nitrogen	200

*All parameters are expressed in mg/L, except pH and temperature (℃).

2.5 Conventional Treatment Systems

Raw POME discharges into nearby watercourses leads to significant environmental issues due to its high content of organics and nutrients (Hassan, Kee and Al-Kayiem, 2013). Nutrients contained in raw POME are nitrogen, phosphorus, potassium, magnesium, and calcium in which induce unnecessary algae growth in aquatic system, and subsequently cause oxygen depletion (Madaki and Seng, 2013). Table 2.8 shows the concentration of nutrients in raw POME. Therefore, treatments of raw POME are necessary to be designed and implemented. Generally, mechanical techniques are used as pre-treatments prior to biological treatments in order to remove SS, such as sieve, sedimentation bed, and filter. Some physico-chemical techniques are also adopted, including coagulation, flocculation, and adsorption (Igwe and Onyegbado, 2007; Salihu and Alam, 2012). Also, oil trap or de-oiling tank is used as pre-treatment of raw POME (Liew, et al., 2015). It is a crucial to ensure that the least quantities of residual oil get into treatment plant without affecting treatment efficiency (Madaki and Seng, 2013).

Table 2.8 Concentration of Nutrients in Raw POME (Ling, 2007)

*Parameter	Concentration
Total Nitrogen	750
Phosphorus	18
Potassium	2,270
Magnesium	615
Calcium	439

*All parameters are expressed in mg/L.

2.5.1 Pond Treatment Systems

Nowadays, more than 85% of palm oil mills in Malaysia adopted ponding systems for biological treatments because of low capital and operating costs, where the rest used open tank digesters (Abdurahman, Azhari and Rosli, 2013; Bala, Lalung and Ismail, 2014; Madaki and Seng, 2013). Ponding systems are normally employed in the palm oil mills as conventional raw POME treatments or stabilization ponds, where long retention time and large treatment area are needed (Bala, Lalung and Ismail, 2014; Rupani et al., 2010). Basically, these systems rely on suitable bacteria to carry out biological degradation in which break down organics, and then reduce BOD of effluent (Madaki and Seng, 2013). A series of ponds for different purposes like anaerobic, facultative as well as aerobic are configured as a biological treatment system. Also, these ponds are made up of earthen structures with no lining (Wong, 2007).

2.5.2 Anaerobic Pond

Anaerobic pond is used prior to facultative or aerobic pond due to its ability to effectively treat high strength wastewater (Igwe and Onyegbado, 2007; Wong, 2007). Besides that, anaerobic digestion has been proved that it is cost effective, environmental sound, minimum sludge formation as well as auxiliary fuel production in form of methane (CH_4) (Madaki and Seng, 2013). However, it has a long hydraulic retention time with minimum of 30 $days$ for organic loading varies from 0.2 - 0.35 $kg\ BOD/m^3/day$, and long start-up period (Bala, Lalung and Ismail, 2014; Wong, 2007). Normally, palm oil mills consist of at least two anaerobic ponds connect in series to receive raw POME for biological degradation. It is often designed as deep pond with 5 - 7 m in depth in which reduces surface area to volume ratio. This design minimises O_2 transfer through air-water interface that is undesirable to upset anaerobic microbes. Three different zones are identified within the anaerobic pond, such as scum, supernatant, and sludge zone. Anaerobic reactions take place at the lowest layer of pond because of anaerobic microbes only active under low or absence of O_2contents, including hydrolysis of biodegradable organics

followed by acidogenesis, acetogenesis, and methanogenesis (Ravindra, 2015; Salihu and Alam, 2012; Wong, 2007). Therefore, biodegradable organics of raw POME are degraded and converted into end-products, such as CH_4, CO_2, trace amounts of hydrogen sulphide (H_2S), and sludge (Madaki and Seng, 2013; Wong, 2007). CH_4 is one of the major compositions of biogas which can be used in electricity generation and saved fossil energy (Rupani et al., 2010).

2.5.3 Facultative Pond

Facultative pond consists of dual microbial degradation zones that are upper aerobic and lower anaerobic zone to further reduce BOD in order to ensure effluent complies with discharge standards (Salihu and Alam, 2012; Wong, 2007). It receives treated POME from anaerobic pond in which settled organics are degraded anaerobically at the bottom layer. Furthermore, remainder of suspended organics are degraded by aerobic or facultative microbes at the upper layer. Both microbes are dominant decomposers in the facultative pond that involve Pseudomonas, Achromobacter, and Flayobacterium. Generally, facultative pond has a shallow pond design with 1 - 1.5 m in depth to maintain a sustainable rate of dissolved O_2. Besides that, facultative pond requires about 8 – 16 $days$ of hydraulic retention time depends upon organic loading and pond depth, but it is shorter than anaerobic pond (Wong, 2007).

2.5.4 Aerobic Pond

Aerobic pond receives treated POME and improves effluent quality from anaerobic pond (Wong, 2007). There are two types of aerobic pond, such as shallow and aerated pond. For the shallow pond, aerobic microbes obtain dissolved O_2 via oxygen transfer between air-water interface and photosynthesis of algae in order to initiate biological degradation. Furthermore, aerated pond is a deep pond that combines with mechanical aeration device to transfer O_2 into and ensure uniform distribution of O_2

throughout the water body (Al-Hashimi and Hussain, 2013; Wong, 2007). On top of that, turbulence effect of aerator has ability to settle some SS, and undergo anaerobic degradation at the bottom layer. About 70 - 90 % of BOD removal efficiency is achieved by using aerobic pond, but effluent may exist in high concentration of SS which induces turbid appearance. Hydraulic retention time of aerobic pond only takes around 8 days which is shorter than anaerobic and facultative pond (Wong, 2007).

2.5.5 Advanced Technologies

Performance of conventional treatments of raw POME can be improved by modifying and introducing advanced technologies. Generally, anaerobic pond has long retention time and start-up period, but both issues can be rectified by using high-rate anaerobic bioreactors as well as granulated seed sludge (Bala, Lalung and Ismail, 2014). The high-rate anaerobic bioreactors include up-flow anaerobic sludge blanket (UASB) reactor, hybrid up-flow anaerobic sludge blanket (HUASB) reactor, and continuous stirred tank reactor (CSTR) (Chong et al., 2012).

UASB reactor is a methane-producing digester which is equipped with granular sludge bed at the bottom part of reactor (Abdurahman, Azhari and Rosli, 2013; Badroldin, 2010). Organics contained in wastewater come in contact with the sludge bed, and are degraded by anaerobic microbes (Abdurahman, Azhari and Rosli, 2013). High performance, short hydraulic retention time, and short start-up period are provided by this reactor (Bala, Lalung and Ismail, 2014; Chong et al., 2012). Therefore, removal efficiency of COD up to 98.4 % is achieved by using UASB reactor for raw POME treatment (Bala, Lalung and Ismail, 2014).

HUASB reactor is usually operated at medium to high organic loading rate of wastewater with COD of 2000 - 20000 mg/L. It is formed by combination of anaerobic filter and granular sludge blanket, where wastewater enters reactor from the bottom and flows upward. Granular sludge blanket is a dense sludge bed in which accumulates large amount of anaerobic microbes at the bottom part of reactor to

breakdown incoming organics through anaerobic digestion. Besides that, anaerobic filter is installed at the top part of reactor, and provides additional treatment of wastewater by retention of sludge granules that escaped from the bottom sludge bed. This reactor is able to provide high COD removal efficiency up to 97 % for raw POME treatment (Badroldin, 2010).

CSTR is a suspended growth system with a configuration of closed-tank digester and mechanical impeller. The impeller provides continuous mixing action in which anaerobic microbes are suspended in the digester, and more contact areas between anaerobic microbes and organics (Bala, Lalung and Ismail, 2014; Hu, 2013). For raw POME treatment, it is capable to achieve about 83 % of COD removal efficiency (Bala, Lalung and Ismail, 2014).

2.6 Post Treatments of Biologically Treated POME

Basically, raw POME is characterized by high concentration of biodegradable organics in nature, and therefore anaerobic, facultative, and aerobic pond are mostly and effectively used in treating raw POME (Aris, et al., 2008). However, conventional raw POME treatments require long hydraulic retention time and only applicable in palm oil mills which have large area of lands (Abdurahman, Azhari and Rosli, 2013; Rupani et al., 2010). Furthermore, biologically treated POME after conventional treatments is quite insufficient to fulfill discharge standards, such as BOD, COD, and SS (Fadzil, Zainal and Abdullah, 2013; Idris, Jami and Muyibi, 2010). Table 2.9 shows the comparison between biologically treated POME and regulatory discharge standards of POME according to EQA 1974. Discharge of ineligible biologically treated POME into nearby watercourses leads to adverse impacts to aquatic life and human health (Fadzil, Zainal and Abdullah, 2013).

Furthermore, effluent colour still intense in dark brown that significantly reduces light penetration into H_2O , and causes unaesthetic view. Low light penetration affects photosynthesis of aquatic plants, and hence suffocation of aquatic organisms occurs because of low O_2 supply (Bello, Nourouzi and Abdullah, 2014;

Fadzil, Zainal and Abdullah, 2013). Unpleasant colour of the effluent is caused by constituents like lignin, phenolic, and repolymerisation of colouring compounds after anaerobic and aerobic treatment (Mohammed and Chong, 2014).

Discharge of high COD effluent into water body results in eutrophication, and subsequently induces oxygen depletion, low water transparency as well as undesirable odour (Fadzil, Zainal and Abdullah, 2013). Oxygen depletion is a phenomenon that fishes or other aquatic organisms encounter suffocation which is caused by severely deprivation of dissolved O_2 from algae, microbes as well as other aquatic plants (Jones-Lee and Lee, 2005).

As such, there is a need of solution by applying post treatment for better effluent quality in order to meet the desirable discharge standards. Post treatments are recommended from several technologies, such as MBR, adsorption, ultrasonic irradiation, and AOP.

Table 2.9 Biologically Treated POME Versus Regulatory Discharge Standards of POME According to EQA 1974 (Fadzil, Zainal and Abdullah, 2013; Lorestani, 2006; Shahrifun et al., 2015)

*Parameter	Biologically Treated POME	Regulatory Discharge Standards
BOD	160	100
COD	1600	1000
SS	14787	400

*All parameters are expressed in mg/L.

2.6.1 MBR

MBR integrates activated sludge process either in aerobic or anaerobic with physical separation by adopting membrane (Azoddein, Haris and Azli, 2015; Bornare et al., 2014). Generally, low pressure membrane filtration either in microfiltration (MF) or ultrafiltration (UF) is used to produce high quality effluent while filtering activated sludge. It is often designed into two different configurations, such as submerged and external (Azoddein, Haris and Azli, 2015; Chong et al., 2012). For the submerged configuration, membrane unit is immersed in the bioreactor in which microbial degradation and physical separation simultaneously take place within same system. Flat sheet or hollow fiber membrane is preferable to be used in submerged configuration. For the external configuration, membrane unit is installed outside the bioreactor, so microbial degradation is prior to physical separation. Installation of high-flow recirculation pump is another external configuration for recirculating activated sludge to bioreactor in order to maintain microbial population. Tubular or spiral-wound membrane is recommended for the external configuration (Frederickson, 2005). Furthermore, submerged configuration has a compact structure and less energy demand that allows it becomes more favourable in the MBR application (Chong et al., 2012).

2.6.2 Adsorption

Adsorption refers as a process that molecules or ions are separated from aqueous solution and adsorbed onto solid surfaces. The solid surfaces acquire energy-rich active sites to interact with adsorbed species in adjacent aqueous phase either in Van der Waals or electrostatic forces (Kandasamy, Vigneswaran and Hoang, 2009; Worch, 2012). All active sites are considered as pores with different sizes and shapes, and classified into micro- ($<2\ nm$), meso- (2 - 50 nm), and macro-pores ($>50\ nm$) (Kandasamy, Vigneswaran and Hoang, 2009). Solid materials provide adsorption surfaces known as adsorbents, where the adsorbed species are referred as adsorbate (Worch, 2012). Adsorption of POME is able to obtain high quality effluent by using commercial powdered activated carbon or zeolite. Furthermore, waste materials are

also considered as potential adsorbents via microwave pyrolysis of rice husk (Zahrim, 2014) or POME sludge in order to produce ash or bio-charcoal.

2.6.3 Ultrasonic Irradiation

Ultrasonic irradiation or sonication is related to a phenomenon that involves formation, growth, and collapse of micro-bubbles in an aqueous solution known as cavitation (Doosti, Kargar and Sayadi, 2012; Nasseri et al., 2006). Cavitation occurs in an extremely short interval of time, within milliseconds (Doosti, Kargar and Sayadi, 2012). Formation of micro-bubbles is developed by intensive compression and rarefaction waves move through aqueous medium in which sufficient to form gas bubbles that consist of H_2O vapour. Subsequently, small gas bubbles absorb ultrasound energy and grow until critical sizes. Beyond the critical sizes, gas bubbles collapse and release large amount of energy (Naddeo et al., 2014). Meanwhile, temperature and pressure increase up to 500 K and 1000 atm, and therefore initiate thermal dissociation of H_2O molecules that lead to formation of $\cdot OH$ with high oxidation potential. Furthermore, $\cdot OH$ quickly react and oxidize organics within the aqueous solution (Doosti, Kargar and Sayadi, 2012).

2.6.4 AOP

AOP is a physico-chemical process that involves two oxidation processes including formation of strong oxidants and reaction of oxidants with organics in wastewater (Kommineni et al., 2008; Vigneswaran, 2008). The strong oxidants mainly refer to $\cdot OH$ that are chemical species with odd number of valence electrons. $\cdot OH$ are generated via transfer of electrons from electron donor to electron acceptor (Kommineni et al., 2008). Besides that, $\cdot OH$ are highly reactive to unselectively react and degrade recalcitrant organics into CO_2 and H_2O, or at least transform into less harmful or biodegradable ones via oxidation or mineralisation (Abdullah, 2008;

Ameta et al., 2012; Chong et al., 2012; Kommineni et al., 2008). Table 2.10 shows the common oxidants used in AOP with respective oxidation potential.

Table 2.10 Common Oxidants Used in AOP with Respective Oxidation Potential (Abdullah, 2008; Barrera-Díaz et al., 2014; Chen, Jhou and Huang, 2014; Martínez-Huitle and Andrade, 2011)

Oxidant	Oxidation Potential, V
Fluorine (F_2)	3.00
$\cdot OH$	2.80
$SO_4^{\cdot -}$	2.60
O_3	2.10
$S_2O_8^{2-}$	2.01
H_2O_2	1.80
Hypochlorite (ClO^-)	1.49
Chlorine (Cl_2)	1.40

Generally, oxidation potential or redox potential of a chemical species refers to tendency to acquire electrons. In which, the higher the oxidation potential, the greater the species to gain electrons. Hence, oxidants are able to induce other species to lose electrons through oxidation that indicates degradation of organics is initiated (Szymczycha and Pempkowiak, 2016). Furthermore, hydrogen abstraction and radical addition are the main chemical reaction mechanisms of the $\cdot OH$ (Abdullah, 2008; Quiroz et al., 2011; Stasinakis, 2008). Hydrogen abstraction refers to hydrogen atoms (H) are abstracted by $\cdot OH$ to generate organic free radicals ($R^{\cdot}$) and H_2O as shown in Equation (2.1) (Abdullah, 2008). Organic free radicals ($HOPhX^{\cdot}$) are also produced via radical addition to double bonds of aliphatic or aromatic compounds as shown in Equation (2.2) (Abdullah, 2008; Quiroz et al., 2011). Both free radicals further react practically with O_2 to form peroxy radicals ($RO_2^{\cdot}$) as shown in Equation (2.3), and subsequently initiate a series of oxidative degradation chain reactions that result in complete oxidation of organics with end products of CO_2 and H_2O (Kapalka, 2008; Khalid, 2011; Quiroz et al., 2011).

$$RH + \cdot OH \rightarrow R^{\cdot} + H_2O \quad (2.1)$$

$$PhX + \cdot OH \rightarrow HOPhX^{\cdot} \quad (2.2)$$

$$R^{\cdot} + O_2 \rightarrow RO_2^{\cdot} \rightarrow CO_2 + H_2O \quad (2.3)$$

Therefore, AOP has potential for treating wastewater with non-biodegradable or hardly biodegradable organics in biologically treated POME (Segneanu et al., 2013). Different available AOP technologies are efficient to treat biologically treated POME which adopt combination of powerful oxidants with catalysts or ultraviolet light, such as hydrogen peroxide photolysis (UV/H_2O_2), ambient-Fenton process (Fe^{2+}/H_2O_2) as well as solar-Fenton process ($Fe^{2+}/H_2O_2/UV$) (Aris et al., 2008; Stasinakis, 2008). Table 2.11 shows the different AOP technologies used in treating biologically treated POME. Table 2.12 shows the comparison between different post treatments used in treating biologically treated POME.

Table 2.11 Different AOP Technologies Used in Treating Biologically Treated POME

Process	Removal Efficiencies	References
Fe^{3+}/H_2O_2	75.2 % of COD 92.4 % of colour	(Aris et al., 2008)
$Fe^{2+}/H_2O_2/UV$	82.4 % of COD 95.1 % of colour	(Aris et al., 2008)
UV/H_2O_2	61.1 % of COD 61.3 % of colour	(Abdullah, 2008)

Table 2.12 Comparison Between Different Post Treatments Used in Treating Biologically Treated POME

Technology	Advantages	Disadvantages	Removal Efficiencies	References
MBR	• Small footprint • High loading rate capability • Producing high quality effluent and disinfection	• Membrane fouling • High capital cost • High running cost	• 58.9 % of COD • 35.3 % of SS • 20.4 % of turbidity	(Azoddein, Haris and Azli, 2015) (Mutamim et al., 2013)
Adsorption	• Good removal of wide variety of dyes (Basic, reactive, and acid dyes)	• Removal is pH dependent • Expensive in regeneration • Adsorbent loss during regeneration	• 41 % of COD • 88 % of color	(Shah, 2014) (Zahrim, 2014)
Ultrasonic Irradiation	• No introduction of additives	• Only feasible on small scale treatment	• 55 % of COD (Ultrasonic Irradiation alone) • 96 % of COD (Combination of Ultrasonic Irradiation and activated carbon)	(Saberi, 2010) (Zahrim, 2014)
AOP	• Forming highly reactive free radicals with strong oxidative power for mineralisation	• Removal is pH dependent • Cost-prohibitive	• 82.4 % of COD • 95.1 % of color	(Shah, 2014) (Zahrim, 2014)

2.7 Electrooxidation

Electrooxidation is an AOP that relies on $OH\cdot$, other ions and radicals in which assist in organics mineralisation (Ahmed, 2008). Electrons are the main and clean reagents in the electrooxidation without creating secondary by-products or pollutants (Morsi, Al-Sarawy and El-Dein, 2011). Meanwhile, high removal efficiencies, simplicity in operations, robustness in configurations, and low temperature requirements are also offered by electrooxidation (Barrera-Díaz et al., 2014; Morsi, Al-Sarawy and El-Dein, 2011; Wang et al., 2012).

Basically, oxidation takes place at anode and reduction occurs at cathode (Wang et al., 2012). Oxidation of organics takes place in two different ways, such as direct and indirect oxidation. For the direct oxidation, organics are adsorbed on the anode surface and degraded by reaction of anodic electrons transfer as shown in Figure 2.2. Indirect oxidation refers to organics are degraded by electrochemically generated oxidants within bulk solution as shown in Figure 2.3 and 2.4 (Barrera-Díaz et al., 2014; Britto-Costa and Ruotolo, 2012). These oxidants can be generated either anodically or cathodically, such as Cl_2 and H_2O_2 which can subsequently lead to formation of $OH\cdot$ and ClO^- (Barrera-Díaz, et al., 2014).

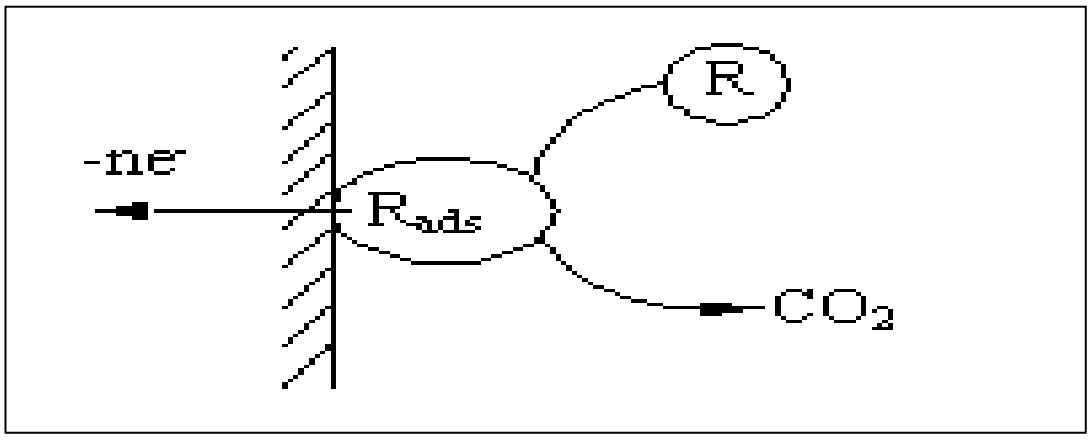

Figure 2.2 Organics Adsorbed on the Anode Surface and Degraded by Anodic Electrons Transfer Reaction (Wang et al., 2012)

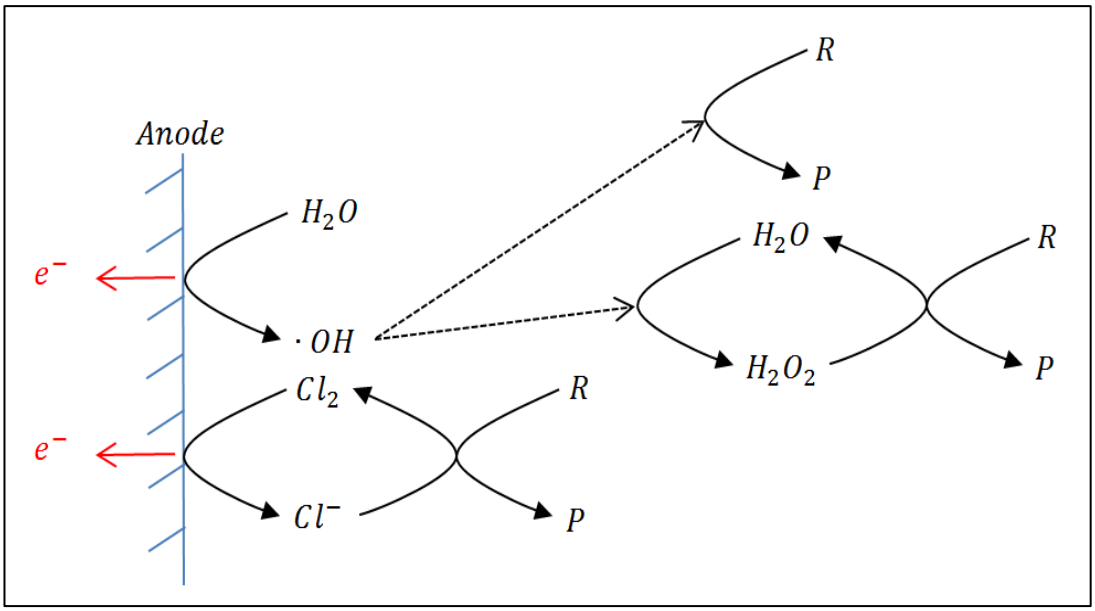

Figure 2.3 Organics Degraded by Electrochemically Generated Oxidants (Anode) within Bulk Solution (Barrera-Díaz et al., 2014; Wang et al., 2012)

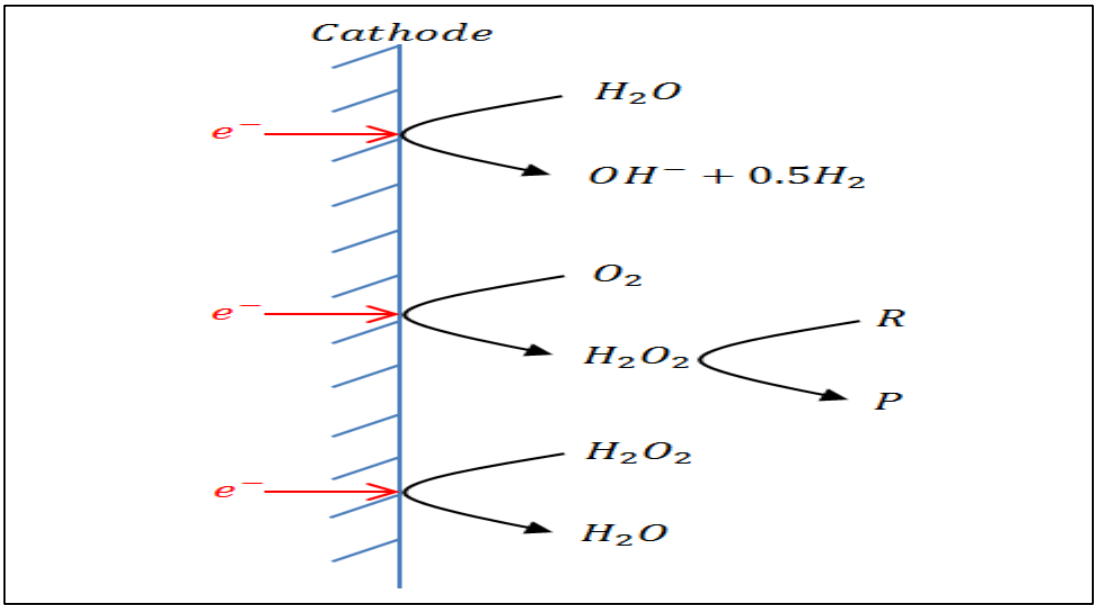

Figure 2.4 Organics Degraded by Electrochemically Generated Oxidants (Cathode) within Bulk Solution (Barrera-Díaz et al., 2014)

Chemical mechanisms of organics degradation on the metal oxide (MO_x) anode are shown below (Feng et al., 2014; Kapalka, 2008; Martínez-Huitle and Andrade, 2011; Morsi, Al-Sarawy and El-Dein, 2011). First of all, H_2O are discharged at the anode to form adsorbed hydroxyl radicals, $MO_x(\cdot OH)$ as shown in Equation (2.4).

$$MO_x + H_2O \rightarrow MO_x(\cdot OH) + H^+ + e^- \quad (2.4)$$

$MO_x(\cdot OH)$ may react with oxygen from the MO_x in which lead to transition of oxygen from $MO_x(\cdot OH)$ to oxide, and form higher oxides (MO_{x+1}) as shown in Equation (2.5).

$$MO_x(\cdot OH) \rightarrow MO_{x+1} + H^+ + e^- \quad (2.5)$$

Both situations result in two different states of "active oxygen" on the anode surface, such as physisorbed $MO_x(\cdot OH)$ and chemisorbed MO_{x+1}. In the presence of oxidisable organics, $MO_x(\cdot OH)$ mainly induce complete combustion of organics and result in formation of CO_2 and H_2O as shown in Equation (2.6). Besides, MO_{x+1} participate in formation of selective oxidation products (RO) through partially oxidation as shown in Equation (2.7).

$$R + MO_x(\cdot OH) \rightarrow Intermediate \rightarrow CO_2 + H_2O \quad (2.6)$$

$$R + MO_{x+1} \rightarrow RO + MO_x \quad (2.7)$$

For the direct and indirect oxidation, O_2 often participate in combustion of organics after formation of $R^{\cdot}$ via hydrogen abstraction as shown in Equation (2.8). Furthermore, $R^{\cdot}$ react with O_2 formed from the anode to generate $RO_2^{\cdot}$ as shown in Equation (2.9), and $RO_2^{\cdot}$ undergo hydrogen abstraction again to form organic hydrogen peroxides ($ROOH$) and another organic radicals as shown in Equation (2.10). Since $ROOH$ are relatively unstable in which continuously decompose to produce intermediates with lower carbon number, and subsequently form CO_2 and H_2O.

$$RH + \cdot OH \rightarrow R^{\cdot} + H_2O \quad (2.8)$$

$$R^{\cdot} + O_2 \rightarrow RO_2^{\cdot} \quad (2.9)$$

$$RO_2^{\cdot} + RH \rightarrow ROOH + R^{\cdot} \quad (2.10)$$

A primary reaction occurs simultaneously with anodic reaction that produces H_2 at the cathode (Mohajeri et al., 2010) as shown in Equation (2.11). Under acidic condition, H_2O_2 are directly generated via oxygen reduction at cathode that supplied mainly from anodic oxidation of H_2O, and subsequently form $\cdot OH$ as shown in Equation (2.12), (2.13), and (2.14) (Barrera-Díaz et al., 2014).

$$2H_2O + 2e^- \leftrightarrow 2OH^- + H_2 \quad (2.11)$$

$$O_2 + 2H^+ + 2e^- \leftrightarrow H_2O_2 \quad (2.12)$$

$$2H_2O \leftrightarrow O_2 + 4H^+ + 4e^- \quad (2.13)$$

$$H_2O_2 + e^- + H^+ \leftrightarrow H_2O + \cdot OH \quad (2.14)$$

2.8 Persulphate

Persulphate is a general term that refers as $S_2O_8^{2-}$ in which originally dissociated from highly soluble $Na_2S_2O_8$ in water (Ocampo, 2009; Padmanabhan, 2008). Besides, $S_2O_8^{2-}$ are non-selectively towards organics, have relatively long life-time, low cost as well as stable at room temperature compared to O_3 and H_2O_2 (Kuśmierek, Świątkowski and Dąbek, 2015; Sun and Wang, 2015). $S_2O_8^{2-}$ are also one of the strong oxidants with oxidation potential of 2.01 V (Abu Amr, Aziz and Adlan, 2013; Ocampo, 2009; Martínez-Huitle and Andrade, 2011). Generally, $S_2O_8^{2-}$ have slow kinetic rate to react with organics, but $S_2O_8^{2-}$ can be activated via electrolysis to accept electrons and generate $SO_4^{\cdot -}$ with oxidation potential of 2.60 V (Chung et al.,

2012; Ocampo, 2009; Padmanabhan, 2008; Wilson et al., 2013) as shown in Equation (2.15). In addition, $S_2O_8^{2-}$ can be regenerated via anodic oxidation of sulphate ions (SO_4^{2-}) as shown in Equation (2.16) (Chen, Jhou and Huang, 2014).

$$S_2O_8^{2-} + e^- \rightarrow SO_4^{\cdot-} + SO_4^{2-} \; or \; 2SO_4^{\cdot-} \tag{2.15}$$

$$SO_4^{2-} \rightarrow S_2O_8^{2-} + 2e^- \tag{2.16}$$

$SO_4^{\cdot-}$ are considered as stronger oxidants compared to $S_2O_8^{2-}$, have fast kinetic rate, more stable than $\cdot OH$, and thus longer-lived in solution (Shi, 2015; Ocampo, 2009). Once $SO_4^{\cdot-}$ are in the solution, radical inter-conversion reactions are initiated to generate $\cdot OH$ (Padmanabhan, 2008) as shown in Equation (2.17).

$$SO_4^{\cdot-} + H_2O \rightarrow SO_4^{2-} + \cdot OH + H^+ \tag{2.17}$$

On top of that, H_2O_2 can be produced via hydrolysis of $S_2O_8^{2-}$ under acidic condition (Chung et al., 2012) as shown in Equation (2.18). Furthermore, H_2O_2 reduction at cathode is capable to produce $\cdot OH$ with oxidation potential of $2.80\,V$ (Barrera-Díaz et al., 2014) as shown in Equation (2.19).

$$S_2O_8^{2-} + 2H_2O \rightarrow H_2O_2 + 2HSO_4^- \tag{2.18}$$

$$H_2O_2 + e^- + H^+ \leftrightarrow H_2O + \cdot OH \tag{2.19}$$

Both $SO_4^{\cdot-}$ and $\cdot OH$ are highly reactive species in which rapidly and unselectively react with organics in a series of chain reactions that result in formation of CO_2 and H_2O as end-products via hydrogen abstraction, addition to double bond, or direct electron transfer as shown in Equation (2.20) to (2.25) (Cronk, 2008; Padmanabhan, 2008; Sun and Wang, 2015; Wilson et al., 2013). On the other hand, $SO_4^{\cdot-}$ ($2.50\,V$ - $3.10\,V$) are predominant and have higher oxidation potential than $\cdot OH$ ($1.80\,V$ – $2.70\,V$) at neutral pH. Under acidic condition, both radicals have same oxidation potential (Padmanabhan, 2008; Sun and Wang, 2015).

Initiation: $$S_2O_8^{2-} + R \rightarrow 2SO_4^{\cdot -} + R^{\cdot} \quad (2.20)$$

Propagation: $$SO_4^{\cdot -} + H_2O \rightarrow HSO_4^{-} + \cdot OH \quad (2.21)$$

Termination 1: $$SO_4^{\cdot -} + RH \rightarrow HSO_4^{-} + R^{\cdot} \quad (2.22)$$

Termination 2: $$\cdot OH + RH \rightarrow H_2O + R^{\cdot} \quad (2.23)$$

Final 1: $$R^{\cdot} + O_2 \rightarrow RO_2^{\cdot} \quad (2.24)$$

Final 2: $$RO_2^{\cdot} + RH \rightarrow ROOH + R^{\cdot} \rightarrow CO_2 + H_2O \quad (2.25)$$

Therefore, synergistic effect of $S_2O_8^{2-}$ is capable to enhance electrooxidation performance via generating several strong oxidants to simultaneously degrade organics in bulk solution (Chen, Jhou and Huang, 2014).

2.9 Electrocoagulation and Electrofloatation

Presence of anode and cathode in electrooxidation leads to another two synergistic processes occur in bulk solution that are electrocoagulation and electrofloatation. Both processes depend on principle of electrical current through electrodes, resulting in different chemical species that are effectively in removing organics, SS as well as heavy metals. For the electrocoagulation, anode serves as "sacrificial" electrode in which M^{n+} are produced via anodic dissolution, and migrate to bulk solution such as aluminium ions (Al^{3+}) as shown in Equation (2.26). Al^{3+} act as destabilising agents to take part in charge neutralisation of pollutants, and subsequently lead to formation of loose aggregates. Furthermore, Al^{3+} also form amorphous aluminium hydroxide ($Al(OH)_3$) through accepting OH^- at the cathode (Bazrafshan, 2008; Rahmalan, 2009) as shown in Equation (2.27). $Al(OH)_3$ have high adsorption properties to bond with destabilised pollutants, and thus forming large lattice-structures or flocs (Kabdaşlı et al., 2012).

$$Al \rightarrow Al^{3+} + 3e^{-} \quad (2.26)$$

$$Al^{3+} + 3OH^{-} \rightarrow Al(OH)_3 \quad (2.27)$$

Electrofloatation mainly depends on formation of H_2 with observation of vigorous bubbling at the cathode as shown in Equation (2.11). Final stage of both processes is removal of trapped pollutants or large flocs either through sedimentation, or H_2 bubbles floatation (Rahmalan, 2009). Figure 2.5 shows the formation of M^{n+}, $M(OH)_n$ as well as H_2 at the anode and cathode.

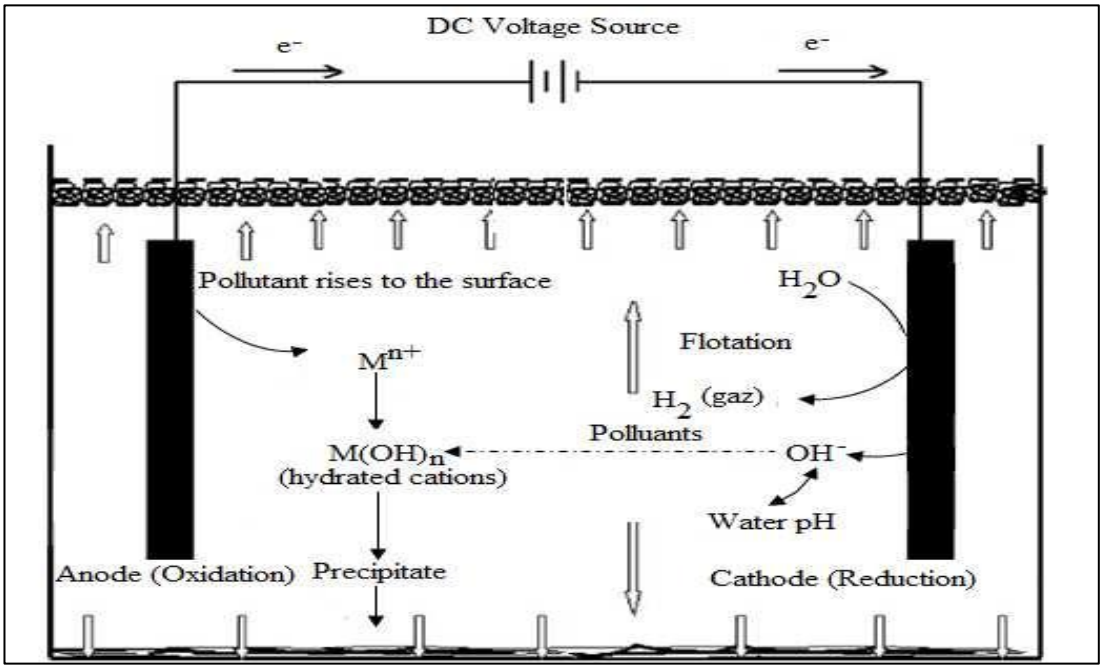

Figure 2.5 Formation of M^{n+}, $M(OH)_n$, and H_2 at Anode and Cathode (Lekhlif et al., 2014)

2.10 Electro Persulphate Oxidation

Electro persulphate oxidation is a process that applies synergistic effect of $S_2O_8^{2-}$ coupled with electrooxidation, electrocoagulation, and electrofloatation as mentioned before. In the past, lacked of researches on treatment of biologically treated POME by using electro persulphate oxidation. Recent studies were carried out which

adopted electro persulphate oxidation to treat dinitrotoluenes (DNTs) and anilines in industrial wastewater (Chen, Jhou and Huang, 2014; Chen and Huang, 2015). Therefore, electro persulphate oxidation was introduced as a post treatment to further treat biologically treated POME to achieve stringent discharge standards for the first time.

2.10.1 Factors Affecting Electro Persulphate Oxidation

There are several factors contribute significant effects on performance of electro persulphate oxidation. Therefore, these factors have to be considered and analysed carefully to avoid unnecessary influence on the electro persulphate oxidation.

2.10.1.1 Electrode

An ideal anodic material should be inexpensive, highly active towards organics degradation, and less active towards oxygen evolution reaction (OER). Both selectivity and efficiency are strongly affected by nature of the anodic material. Anodic material can be categorized into active and non-active anode. Active anode has low oxygen evolution over-potential and acts as good electro-catalyst for the OER that leads to partial oxidation of organics (Martínez-Martínez-Huitle and Andrade, 2011). First of all, H_2O are discharged at anode to form $MO_x(\cdot OH)$ (Morsi, Al-Sarawy and El-Dein, 2011) as shown in Equation (2.4).

Furthermore, OER is induced by oxidation of H_2O that results in formation of O_2, and converts $MO_x(\cdot OH)$ back to surface sites, $MO_x(\quad)$ (Martínez-Martínez-Huitle and Andrade, 2011) as shown in Equation (2.28). Thus, less $MO_x(\cdot OH)$ to react and degrade organics.

$$MO_x(\cdot OH) + H_2O \rightarrow MO_x(\quad) + O_2 + 3H^+ + 3e^- \qquad (2.28)$$

Subsequently, only MO_{x+1} participate in partially oxidation of organics at the anode, and form selective oxidation products (Morsi, Al-Sarawy and El-Dein, 2011) as shown in Equation (2.7).

On the other hand, non-active anode is poor electro-catalyst with high oxygen evolution over-potential in which $\cdot OH$ weakly interact with anode surface, but directly oxidize organics in very small distance to anode. This situation is considered as "almost" direct oxidation, and forms CO_2 and H_2O as shown in Equation (2.6) (Barrera-Díaz et al., 2014; Martínez-Martínez-Huitle and Andrade, 2011).

Generally, aluminium or iron electrode is selected and used in electrocoagulation (Ali and Yaakob, 2012). Ferrous ions (Fe^{2+}) produced from iron electrode are easily oxidised to ferric ions (Fe^{3+}), and subsequently lead to formation of ferric hydroxides ($Fe(OH)_3$). However, $Fe(OH)_3$ are fine particles and difficult to precipitate, and thus aluminium electrode is preferred because of effectively trapping organics, (SS), and heavy metals (Nasrullah, Singh and Wahid, 2012).

2.10.1.2 Current Density

Current density is an important variable that affects organics degradation in electro persulphate oxidation. Degradation of organics tends to be improved by increasing current density because of more $MO_x(\cdot OH)$ are formed at anode as well as $\cdot OH$ in bulk solution (González-Vargas, Salazar and Sirés, 2014; Kariyajjanavar, Narayana and Nayaka, 2011). However, further increase in current density shift cathode potential to an unfavourable value that causes cathodic reduction of O_2 to form H_2O_2 (González-Vargas, Salazar and Sirés, 2014). Excessive formation of H_2O_2 brings negative interference on COD test. Meanwhile, high energy consumption is needed at high current density that is not preferable (Kariyajjanavar, Narayana and Nayaka, 2011). Increasing current density during electro persulphate oxidation, more $SO_4^{\cdot-}$ are

formed in the bulk solution to simultaneously increase organics mineralisation as well (Chen, Jhou and Huang, 2014).

According to Faraday's Law, increasing current density is able to generate more M^{n+} like Al^{3+} in the solution. Al^{3+} act as destabilising agents to promote charge neutralization or destabilisation of pollutants (Ozyonar and Karagozoglu, 2012; Ni'am et al., 2007; Rahmalan, 2009). Also, aluminium hydroxide $Al(OH)_3$ are formed by reaction between Al^{3+} and OH^- produced at cathode, and therefore trap destabilised pollutants to form large flocs which can be removed via sedimentation or floatation. Furthermore, increasing production rate of H_2 bubbles and decreasing size of bubbles at the cathode are triggered by high current density (Ozyonar and Karagozoglu, 2012). Hence, high surface area per unit volume of gas is promoted by small bubbles to allow more trapped pollutants to attach and float (Mickova, 2015).

2.10.1.3 Contact Time

Contact time is directly proportional to organics mineralisation. When the contact time increases, more $MO_x(\cdot OH)$ are formed at anode, and more $\cdot OH$ and $SO_4^{\cdot -}$ are generated in bulk solution to react and degrade organics (Jumaah and Othman, 2015; Khandegar and Saroha, 2012; Zhu et al., 2014). After certain contact time, mineralisation rate is slowed down because of oxidation reaction becomes more complex with slow reaction speed, so removal efficiency may be slightly increased (Zhu, et al., 2014). On top of that, further increase in contact time leads to high electrical energy consumption which is not preferable (Jumaah and Othman, 2015).

Furthermore, increasing contact time in electrocoagulation and electrofloatation leads to high generation rate of M^{n+} and OH^- (Nasrullah, Singh and Wahid, 2012). Subsequently, more reactions between M^{n+} and OH^- can form more $M(OH)_n$, such as $Al(OH)_3$ which have high adsorption properties to bond with destabilised pollutants, and form large lattice-structures (Kabdaşlı et al., 2012).

Besides that, high production of OH^- at cathode indicates increasing amount of H_2 bubbles which allow more trapped pollutants to attach and float as well.

2.10.1.4 Initial pH

Initial pH is one of the factors that affect mineralisation in electro persulphate oxidation. Normally, mineralisation efficiency increases from alkaline to acidic condition (Bonyadinejad et al., 2015; Chen and Huang, 2015). Under low pH value, oxygen evolution over-potential increases to minimise anodic OER, and leads to formation of more $MO_x(\cdot OH)$ at anode as well as $\cdot OH$ in bulk solution which are responsible for organics degradation (Bonyadinejad et al., 2015). At the same time, generation of H_2O_2 via oxygen reduction at cathode is reduced under stronger acidic condition in order to avoid unnecessary disturbance on COD test (Chen and Huang, 2015).

Under high pH value, $SO_4^{\cdot -}$ react with OH^- to form $\cdot OH$, and further dissociate into oxide radicals ($O^{\cdot -}$) with low oxidation potential which decrease mineralisation rate as shown in Equation (2.29) and (2.30) (Bonyadinejad et al., 2015; Sogaard, 2014).

$$SO_4^{\cdot -} + OH^- \rightarrow SO_4^{2-} + \cdot OH \quad (2.29)$$

$$\cdot OH \rightarrow O^{\cdot -} + H^+ \quad (2.30)$$

On the other hand, initial pH has a strong influence on electrocoagulation, especially the formation of $M(OH)_n$, such as $Al(OH)_3$. Generally, $Al(OH)_3$ act as chemical species that are predominant at pH 4 to 9.5 (Jotin, Ibrahim and Halimoon, 2012). Based on Figure 2.6, increasing pH tends to form more $Al(OH)_3$, leading to more effective treatment. pH of solution is increased because of increasing OH^- concentration at cathode as shown in Equation (2.11) (Rahmalan, 2009). Size of bubbles is a factor affecting electrofloatation, where small bubbles promote large

surface area per unit volume of gas in order to join more trapped pollutants, and thus float to top surface of solution. Basically, smallest H_2 bubbles with 16 μm in diameter are produced at pH 3 to 4 (Mickova, 2015).

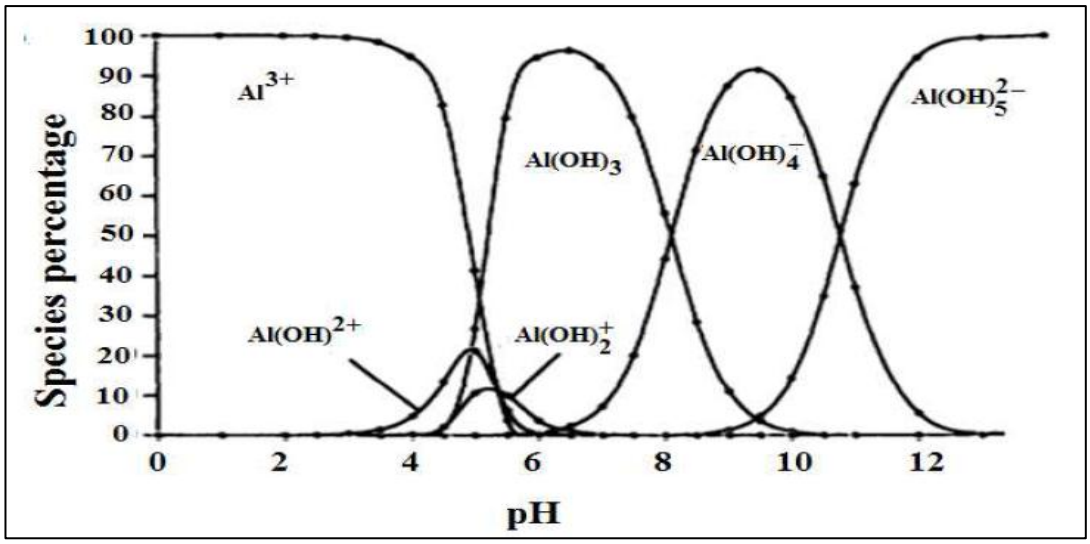

Figure 2.6 Aluminium Hydroxide Species at Different pH (Lekhlif et al., 2014)

2.10.1.5 $S_2O_8^{2-}$ Dosage

Initially, increment of $S_2O_8^{2-}$ dosage leads to formation of more $SO_4^{\cdot-}$ via cathodic reduction of $S_2O_8^{2-}$, and increases organics mineralisation. However, destruction efficiency tends to be decreased because of amounts of $S_2O_8^{2-}$ are reduced after certain period of time. Since less competitive adsorption between $S_2O_8^{2-}$ and O_2 at cathode in which promotes formation of H_2O_2 via oxygen reduction (Chen, Jhou and Huang, 2014). Meanwhile, increase in $S_2O_8^{2-}$ can induce more H_2O_2 formation via hydrolysis under acidic condition (Chen and Huang, 2015; Chung et al., 2012). Excessive formation of H_2O_2 brings negative effect on COD test. This is because H_2O_2 react with dichromate ions ($Cr_2O_7^{2-}$) in which reduce amounts of $Cr_2O_7^{2-}$ required to convert organics into CO_2 and H_2O (Talinli and Anderson, 1992). Besides, H_2O_2 have lower oxidation potential than $SO_4^{\cdot-}$ that also reduce the mineralisation efficiency. Therefore, optimum $S_2O_8^{2-}$ dosage should be taken into consideration to ensure a desirable performance and remain economic.

2.11 Design-Expert® (DOE)

Several operational variables such as current density, contact time, initial pH as well as $S_2O_8^{2-}$ dosage have a great effect on removal and process efficiencies. In order to ensure a promising treatment system and maintain a desirable economic design, RSM provided by DOE software version 10.0 should be adopted to experimentally determine optimum operational conditions.

DOE is normally employed with purpose of experimental design, modeling, and optimisation. It promotes several programs include full factorial and fractional factorial designs, RSM, mixing and D-optimal designs. Experimental design refers to specific sets of experiment defined by different combinations of operational variable values. Operational variables are also known as independent variables, where responses are measured values from experiments or dependent variables (Bashir et al., 2015).

CHAPTER 3

METHODOLOGY

Figure 3.1 shows a methodology flowchart that describes all processes from initial collection of biologically treated POME to report writing. First of all, biologically treated POME was collected from Tian Siang Oil Mill (Air Kuning) Sdn Bhd. Initial characteristics of biologically treated POME for example, COD, BOD, colour, turbidity, pH, SS, $NH_3 - N$, and heavy metals were tested according to standard methods (APHA, 2005; HACH 2005). Subsequently, preliminary experiments were conducted to study effect of $S_2O_8^{2-}$ dosage on the performance of electrooxidation. Based on preliminary experimental results, DOE was used to generate different sets of operational variable values for conducting experiments. Moving on, results obtained from the experiments were analysed and optimised via RSM. Moreover, validation process and cost estimation were carried out, and then started in report writing.

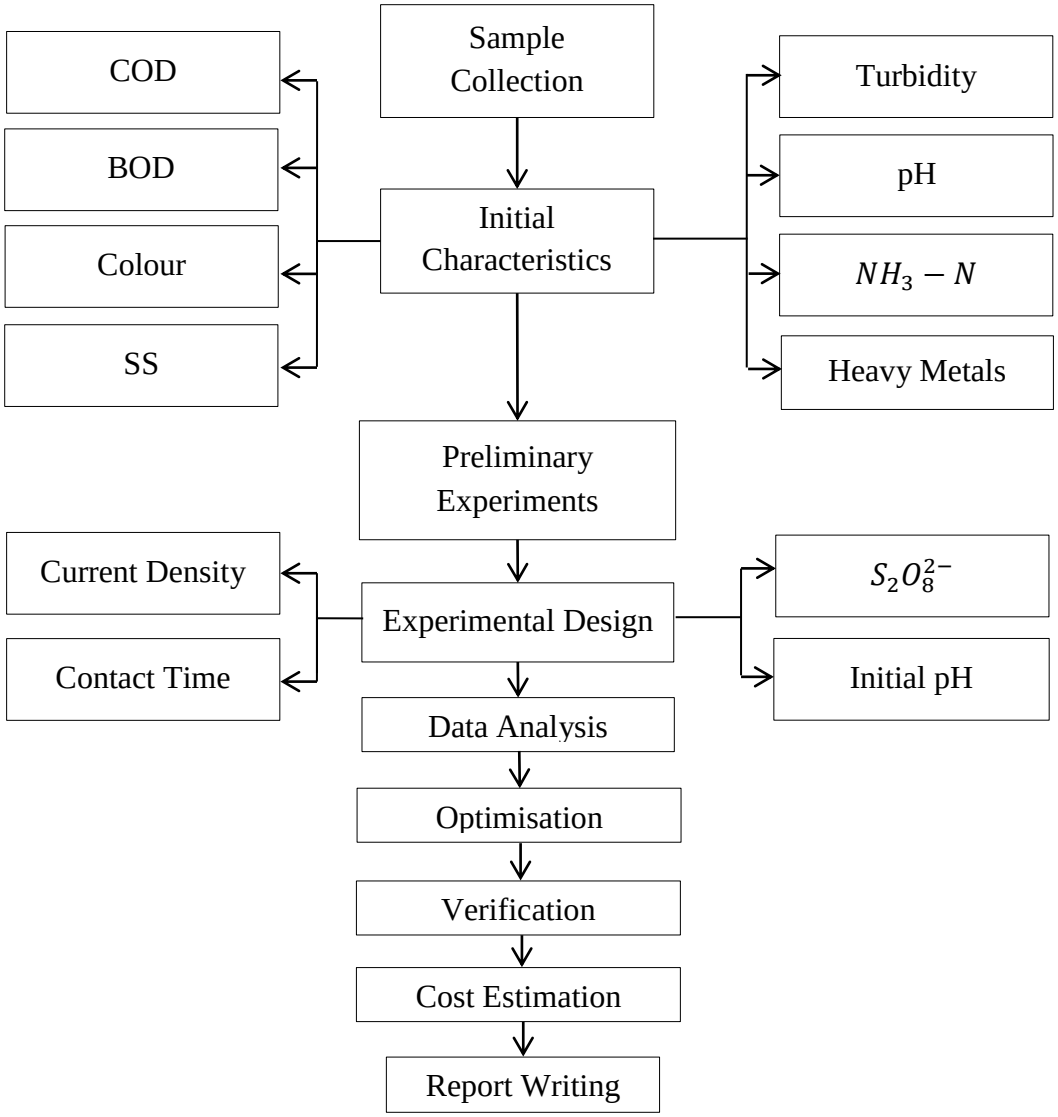

Figure 3.1 Methodology Flowchart

3.1 Location of Biologically Treated POME Collection

Biologically treated POME was collected from Tian Siang Oil Mill (Air Kuning) Sdn Bhd. The location was placed at District of Batang Padang, Perak, and required to travel around 22.8 km from Universiti Tunku Abdul Rahman (UTAR) Perak Campus as shown in Figure 3.2. This mill was developed in year 2000, and its FFB processing capacity had expanded from 60 to 120 $tons/hr$. Tank digesters and ponding systems were adopted in this mill, and total of 11 ponds available for aerobic biological treatments of treated POME from anaerobic digester tanks. The collection of biologically treated POME was done at aerobic pond number 10 by using several empty bottles with 5.5 L of capacity as shown in Figure 3.3 and 3.4. Furthermore, the collected biologically treated POME was then sent to environmental laboratory, and stored in laboratory refrigerator at 4 ℃ to minimise any occurrences of biological or chemical reactions (APHA, 2005).

Figure 3.2 Distance Traveled from UTAR Perak Campus to Tian Xiang Oil Mill (Air Kuning) Sdn Bhd

Figure 3.3 Collection of Biologically Treated POME at Aerobic Pond Number 10

Figure 3.4 Collection of Biologically Treated POME with 5.5 *L* Bottle

3.2 Biologically Treated POME Characteristics

Generally, characteristics of biologically treated POME are represented by COD, BOD, colour, SS, turbidity, pH, $NH_3 - N$, and heavy metals. These characteristics are important and useful in design of wastewater treatment. Hence, Standard Methods for the Examination of Water and Wastewater and Hach Water Analysis Handbook were adopted in analysis of characteristics (APHA, 2005; Hach, 2005).

3.2.1 COD

COD is commonly used as a parameter to measure amount of organics in POME, and expressed in mg/L. In this study, Dichromate Reactor Digestion Method (HACH Method 8000) was adopted for COD measurement (HACH, 2005). Several equipment are required for determination of COD, such as COD reactor (DRB 200, USA) and UV-Vis spectrophotometer (DR 6000, USA) as shown in Figure 3.5 and 3.6. The COD reactor is preheated to 150 ℃ before putting in any samples. 2 ml of diluted POME sample is pipetted into HR COD Digestion Reagent Vial with an angle of 45°. Furthermore, the vial is inverted gently few times for well mixing, and then heated in the COD reactor for 2 hours. Meanwhile, a HR COD Digestion Reagent Vial is filled with 2 ml of deionized water, a blank solution, and heated in the COD reactor as well. After that, vials are taken out and allowed to cool down to room temperature. Appropriate program code of COD measurement is selected, 435 COD HR, and set the spectrophotometer's reading as zero beforehand by using the blank solution. Lastly, COD value of diluted POME sample is measured in duplicate in order to obtain accurate result, and reading is shown in unit of mg/L.

Figure 3.5 COD Reactor (DRB 200, USA)

Figure 3.6 UV-Vis Spectrophotometer (DR 6000, USA)

3.2.2 BOD

BOD refers to amount of dissolved O_2 required by aerobic microbes for organics degradation and amount of biodegradable organics present in POME. 5-days BOD test (BOD_5) at 20 ℃ is commonly conducted to determine BOD value which is expressed in mg/L (APHA, 2005). POME sample is initially diluted with suitable

dilution factor, then filled into a 300ml BOD bottle and measured initial dissolved O_2 (DO_0) by using DO Meter (EUTECH DO 6+, SINGAPORE) as shown in Figure 3.7. Next, BOD bottle is placed in BOD incubator (FOC 225E, VELP SCIENTIFICA, ITALY) at 20 ℃ as shown in Figure 3.8. After 5 days, BOD bottle is taken out to measure final dissolved O_2 (DO_5). The BOD_5 is calculated by using Equation 3.1.

$$BOD_5 = Dilution\ Factor(DO_0 - DO_5) \quad (3.1)$$

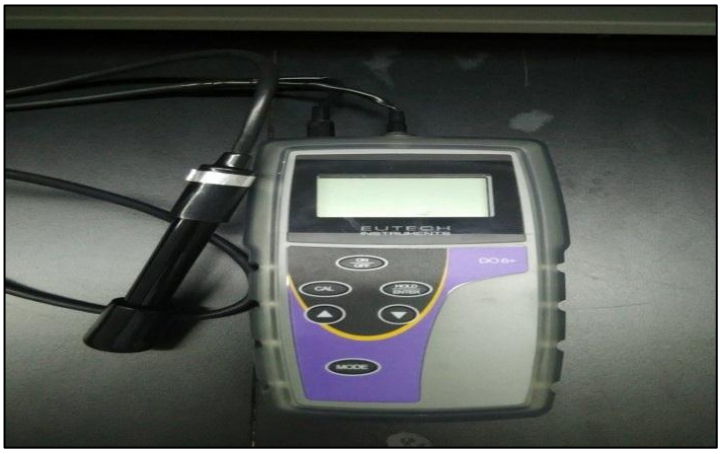

Figure 3.7 DO Meter (EUTECH DO 6+, SINGAPORE)

Figure 3.8 BOD Incubator (FOC 225E, VELP SCIENTIFICA, ITALY)

3.2.3 $NH_3 - N$

$NH_3 - N$ is one of the parameters to determine amount of ammonia in POME. POME sample is initially diluted with an appropriate dilution factor, and then 25 ml of diluted sample is pipetted out for subsequent steps. According to Nessler method, 3 drops of mineral stabilizer are first added into diluted sample and 25 ml of deionized water as blank solution, followed by 3 drops of polyvinyl alcohol and l ml of Nessler reagent (APHA, 2005). Appropriate program code of $NH_3 - N$ measurement is selected, 380 N Ammonia Ness, and set spectrophotometer's reading as zero beforehand by using the blank solution. Lastly, $NH_3 - N$ value of diluted POME sample is measured in duplicate in order to obtain accurate result, and reading is shown in unit of mg/L. Figure 3.9 shows the Nessler reagent, polyvinyl alcohol, and mineral stabilizer.

Figure 3.9 Nezzler Reagent, Polyvinyl Alcohol, and Mineral Stabilizer

3.2.4 pH

pH meter (HANNA HI 2550, ITALY) as shown in Figure 3.10 is used to determine initial and final pH of POME sample through Electrometric Method (APHA, 2005). Calibration of the pH meter is a necessary procedure by using buffer solution with pH 4, 7, and 10 respectively. Besides, pH probe must be rinsed with distilled water before and after measurement. Each measurement is taken until a stable reading shows on the pH meter.

Figure 3.10 pH Meter (HANNA HI 2550, ITALY)

3.2.5 Colour

Spectrophotometric Method-Single Wavelength Method is commonly adopted to measure colour with unit of Platinum-Cobalt ($PtCo$), where a proper dilution is needed to ensure all readings fall within spectrophotometer's range of 0 - 500 units (APHA, 2005). A blank solution is prepared by filling deionized water into empty glass vial. Spectrophotometer's reading is first set as zero by using the blank solution after selecting program code 125 Colour (465 nm wavelength) in order to avoid effect of previous reading, followed by colour measurement of diluted POME sample. Each measurement is conducted in duplicate in order to obtain accurate result.

3.2.6 Turbidity

Turbidity of the POME sample is directly measured by using turbidity meter (LOVIBOND TB 210 IR, GERMANY) through Nephelometric Method as shown in Figure 3.11, where this model provides range of 0.01 – 1100 NTU (APHA, 2005). Calibration is important to be carried out by using four different bottle solutions with < 0.1, 20, 200, and 800 NTU. Each bottle requires to calibrate for 1 minute and stores each reading respectively. Then, POME sample is filled in a 10 ml sample cell and directly measured in duplicate. The unit of reading is shown in Nephelometric Turbidity Unit (NTU).

Figure 3.11 Turbidity Meter (LOVIBOND TB 210 IR, GERMANY)

3.2.7 SS

HACH Method 8006 was used to measure amount of SS in POME sample (HACH, 2005). A blank solution is prepared by filling deionized water into empty glass vial. Besides, POME sample is also filling directly into empty glass vial. Appropriate program code of SS measurement is selected, 630 Suspended Solids, and set spectrophotometer's reading as zero beforehand by using the blank solution. Lastly,

SS value of POME sample is measured in unit of mg/L. Each measurement is conducted in duplicate in order to obtain accurate result.

3.2.8 Heavy Metals

Heavy metals containing in POME sample are analyzed by using Inductively Coupled Plasma Mass Spectrometry (ICP-MS PERKIN ELMER NEXION™ 300Q, USA) as shown in Figure 3.12, such as aluminium (Al), chromium (Cr), iron (Fe), nickel (Ni), lead (Pb), and zinc (Zn). POME sample is initially diluted with an appropriate dilution factor to ensure all readings fall within the ICP-MS's range, followed by adding 1 % of nitric acid (HNO_3). Before analysis, ICP-MS is calibrated by using stock solutions (50 ppb, 100 ppb, 500 ppb, and 1000 ppb) and blank solution (Ultrapure water). Furthermore, sample is labeled and keyed into computer which is connected to ICP-MS. Sample is then tested, and subsequently all tested data are saved in the computer database.

Figure 3.12 Inductively Coupled Plasma Mass Spectrometry (ICP-MS PERKIN ELMER NEXION™ 300Q, USA)

3.3 Experimental Setup

Two aluminium plates are used as anode and cathode with dimension of 12 $cm \times$ 4.5 cm. Only 6 cm of each electrode length is immersed in 500 ml of biologically treated POME, and therefore contact area of 27 cm^2 is provided. Besides that, agitation speed is fixed at 300 revolutions per minute (rpm) to provide a homogeneous mixing within the POME sample. Distance between two electrodes is set as 3 cm apart to each other for maintaining appropriate movement of ions or radicals (Khandegar and Saroha, 2012). Furthermore, a DC power supply (MEGURO MP 303-3, JAPAN) is used to consistently provide electrical current for electro persulphate oxidation. Moving on, entire process is conducted with a set duration. After that, treated POME sample is allowed to settle in order to obtain supernatant, and then several parameters are tested according to Standard Methods for the Examination of Water and Wastewater and Hach Water Analysis Handbook (APHA, 2005; HACH, 2005). Figure 3.13 shows the experimental setup of electro persulphate oxidation.

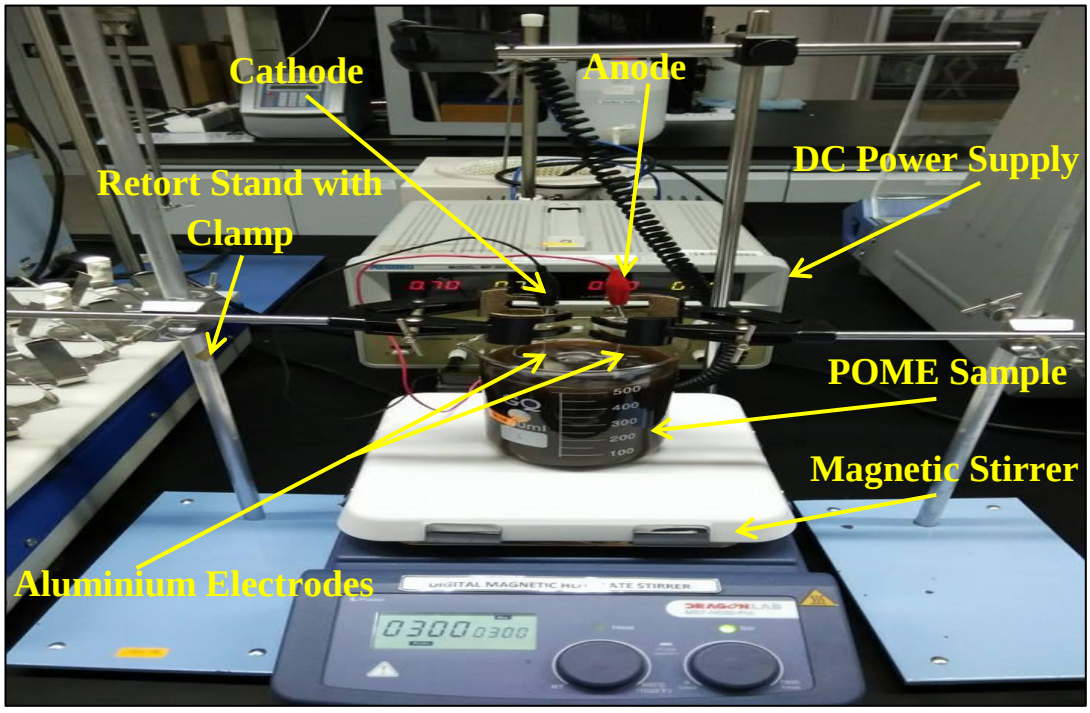

Figure 3.13 Experimental setup

3.4 Preliminary Experiments

Preliminary experiments were conducted in two different stages. First stage was a verification process that employed optimum operational variable values done by previous study, such as current density, contact time, and initial pH to determine and compare COD and colour (Tham, 2015).

Second stage, different $S_2O_8^{2-}$ dosages were added into biologically treated POME to determine and study effect of $S_2O_8^{2-}$ on COD and colour removal. Minor adjustment on current density and contact time were carried out in this stage, and initial pH was adjusted to pH 3. Purpose of both stages was to determine suitable ranges of operational variables, and apply in DOE.

3.5 Experimental Design and Optimisation by Using RSM

Central Composite Design (CCD) is commonly used in RSM for experimental design. CCD is suitable for sequential experiments and testing of lack-of-fit by using a reasonable amount of design points. A total of 30 experiments were designed according to 16 factorial experiments, 8 axial experiments on axis at a distance of $\pm \alpha$ from center, and 6 replicas at center points to assess random error (Bashir et al., 2016). Estimation of linear in response surface can be obtained through factorial experiments. Center points refer to all factors are set to center level respectively, and are replicated in order to enhance experimental precision (Asaithambi, Aziz and Daud, 2016). In addition, center points augmented with axial points to allow estimation of curvature in response surface. CCD consists two models that are first- and second-order model. First-order model is only able to describe linear response surface, so it is not suitable for analysing maximum, minimum, and ridge line (Bradley, 2007). In this study, second-order model was selected as it involved all terms in first-order, all quadratic and interaction terms, such as $\beta_{jj}x_i^2$ and $\beta_{ij}x_ix_j$. It is also known as a quadratic model that describes curving response surface and more precise than first-order model (Asaithambi, Aziz and Daud, 2016). Based on

preliminary results, respective range of operational variables was set and keyed in DOE in order to generate a series of operational variables with different combinations for conducting experiments as shown in Table 3.1 and 3.2.

In this study, RSM was used to determine optimum operational conditions. Mathematical and statistical methods are adopted by RSM for analysing effects of several operational variables on one or more responses in order to obtain maximum benefits from treatment processes. The maximum benefits refer to increasing process efficiency without increasing relevant cost, and ensuring desirable removal efficiency. Optimisation refers to selection of the best elements among the operational variables, while achieving maximum benefits. Therefore, using RSM in experimental optimisation can contribute significant improvement in removal efficiency and operational cost reduction (Bashir et al., 2015).

Table 3.1 Respective Range of Operational Variables

Operational Variable	Range
Current Density	20 – 50 mA/cm^2
Contact Time	10 – 60 min
Initial pH	3 – 5
$S_2O_8^{2-}$ Dosage	0.5 - 4 g

Table 3.2 Experimental Design Matrix

Run	Current Density, mA/cm^2	Contact Time, min	Initial pH	$S_2O_8^{2-}$ Dosage, g	COD Removal, %	Colour Removal, %	SS Removal, %
15	20.00	10.00	3.00	0.50			
29	20.00	10.00	3.00	4.00			
27	20.00	10.00	5.00	0.50			
21	20.00	10.00	5.00	4.00			
23	20.00	60.00	3.00	0.50			
17	20.00	60.00	3.00	4.00			
16	20.00	60.00	5.00	0.50			
8	20.00	60.00	5.00	4.00			
14	27.50	35.00	4.00	2.25			
1	35.00	22.50	4.00	2.25			
18	35.00	35.00	3.50	2.25			
11	35.00	35.00	4.00	1.38			
6	35.00	35.00	4.00	2.25			
30	35.00	35.00	4.00	2.25			
10	35.00	35.00	4.00	2.25			
9	35.00	35.00	4.00	2.25			
25	35.00	35.00	4.00	2.25			
19	35.00	35.00	4.00	2.25			
3	35.00	35.00	4.00	3.13			
4	35.00	35.00	4.50	2.25			
5	35.00	47.50	4.00	2.25			
20	42.50	35.00	4.00	2.25			
12	50.00	10.00	3.00	0.50			
2	50.00	10.00	3.00	4.00			
28	50.00	10.00	5.00	0.50			
7	50.00	10.00	5.00	4.00			
26	50.00	60.00	3.00	0.50			
22	50.00	60.00	3.00	4.00			
24	50.00	60.00	5.00	0.50			
13	50.00	60.00	5.00	4.00			

CHAPTER 4

RESULT AND DISCUSSION

4.1 Initial Characteristics of Biologically Treated POME

Biologically treated POME was unfrozen to room temperature before conducting initial parameter tests. All parameters are tested according to standard methods (APHA, 2005; HACH 2005). Table 4.1 shows the initial characteristics of biological treated POME. Majority of hardly or non-biodegradable organics contained in the POME sample were indicated by high average value of COD, $2420 \pm 100\, mg/L$ than BOD, $60 \pm 5\, mg/L$. Colour of the POME sample stilled intense in dark brown because of high initial measurement with $5240 \pm 400\, PtCo$. Other parameters such as SS, turbidity, $NH_3 - N$, pH, and temperature were also determined in average value respectively, $352 \pm 12\, mg/L$, $639 \pm 11\, NTU$, $53 \pm 3\, mg/L$, $8.5 \pm 0.1\, mg/L$, and $24.8 \pm 0.5\, mg/L$. Table 4.2 shows the initial concentrations of heavy metals in the biologically treated POME.

Table 4.1 Initial Characteristics of Biologically Treated POME

Parameters	Range	Average
BOD	55 – 65	60
COD	2320 – 2520	2420
SS	340 – 364	352
Turbidity	628 – 650	639
$NH_3 - N$	50 – 56	53
Colour	4840 - 5640	5240
pH	8.4 – 8.6	8.5
Temperature	24.3 – 25.3	24.8

*****All parameters are expressed in mg/L, except pH, colour ($PtCo$), temperature (℃) and turbidity (NTU).

Table 4.2 Initial Concentrations of Heavy Metals in the Biologically Treated POME

*Parameter	Concentration
Al	10.695
Cr	3.015
Fe	101.881
Ni	1.263
Zn	51.281
Pb	0.551

*****All parameters are expressed in ppb.

4.2 Preliminary Results

Purpose of preliminary experiments is to determine suitable range of operational variables in which used in subsequent experiments of electro persulphate oxidation, including current density, contact time, initial pH, and $S_2O_8^{2-}$ dosage. First set of the

preliminary experiment was a verification process that applied optimum operational variables obtained from previous study to determine and compare COD and colour removal. These variables were 56 mA/cm^2 of current density, 65 min of contact time, and pH 4.5 (Tham, 2015). As summarized in Table 4.3, COD and colour removal achieved almost same as results in the previous study.

Table 4.3 Verification of COD and Colour Removal Based on Literature (56 mA/cm^2 of Current Density, 65 min of Contact Time, and pH 4.5)

Parameter	Removal Efficiencies, % (Literature)	Removal Efficiencies, % (Verification)
Colour	100.00	98.63
COD	75.40	78.45

Second set of the preliminary experiment was to study effect of different $S_2O_8^{2-}$ dosages in electrooxidation with minor adjustment on current density and contact time to 26 mA/cm^2 and 45 min. Purpose of the adjustment was to determine any different in removal efficiencies with less electrical current and contact time. Meanwhile, initial pH was adjusted to pH 3 for determining effect of this operational variable as well. Through experiments, $S_2O_8^{2-}$ dosage increased from 0.7908 g to 1.5815 g, COD removal was slightly increased from 76.34 % to 78.05 %. However, removal efficiency of COD was dropped to 67.05 % when $S_2O_8^{2-}$ dosage further increased to 3.9537 g as shown in Figure 4.1. This situation indicated that excessive $S_2O_8^{2-}$ dosage could retard COD removal. On the other hand, colour removal was almost same within range of 97.00 % to 98.00 % when $S_2O_8^{2-}$ dosage increased from 0.7908 g to 3.9537 g as shown in Figure 4.2. Due to effect of $S_2O_8^{2-}$, minor adjustment was proved that reduction of current density and contact time could remain good removal and improve process efficiencies. In addition, adjustment of initial pH denoted its effect to maintain good performance of electro persulphate oxidation.

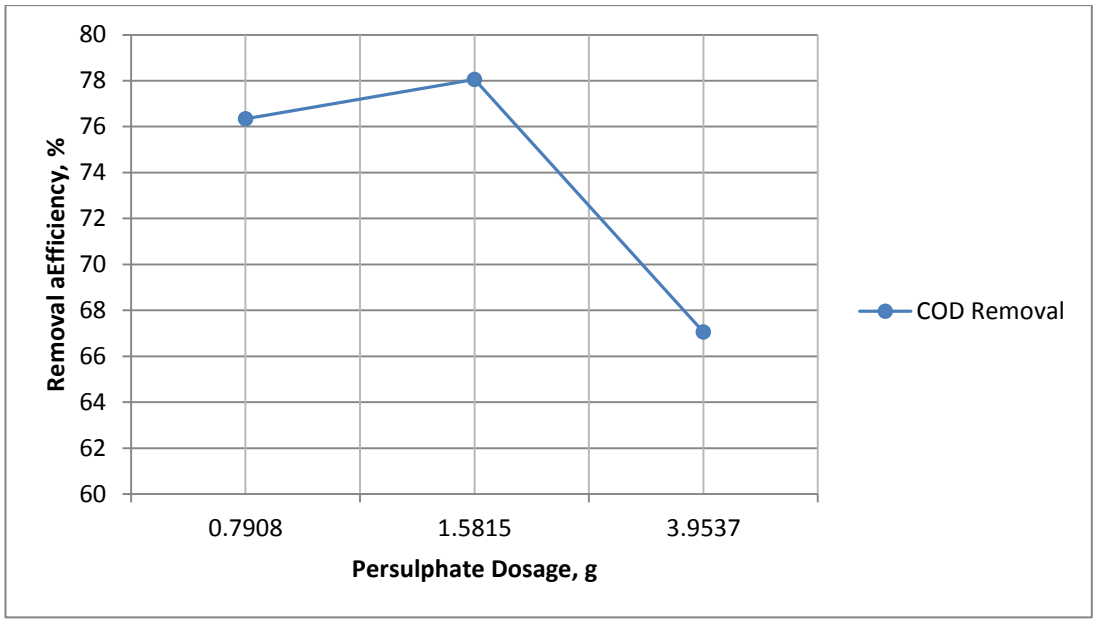

Figure 4.1 Effect of $S_2O_8^{2-}$ on COD Removal

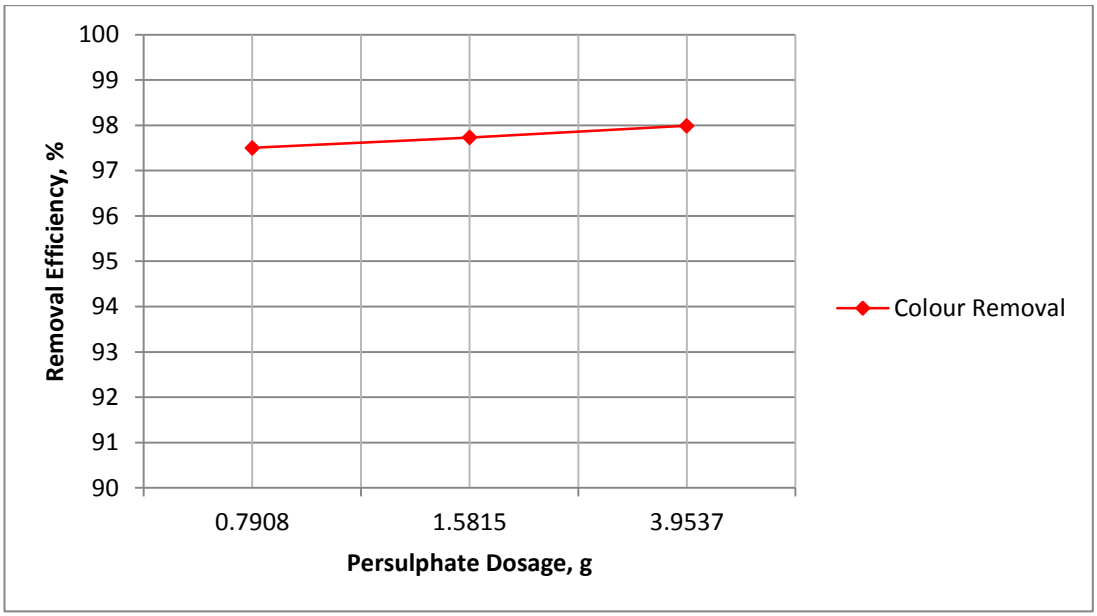

Figure 4.2 Effect of $S_2O_8^{2-}$ on Colour Removal

4.3 Experimental Results

Based on preliminary results, respective range of operational variables was set, and keyed in DOE to generate a total of 30 experiments. After finished 30 runs of experiment, all corresponding removal efficiencies were inserted in respective set of operational variables as shown in Table 4.4.

Table 4.4 Experimental Results

Run	Current Density, mA/cm^2	Contact Time, min	Initial pH	$S_2O_8^{2-}$ Dosage, g	COD Removal, %	Colour Removal, %	SS Removal, %
15	20.00	10.00	3.00	0.50	66.41	66.44	71.12
29	20.00	10.00	3.00	4.00	54.12	68.69	77.35
27	20.00	10.00	5.00	0.50	65.23	52.71	58.52
21	20.00	10.00	5.00	4.00	53.08	63.42	70.13
23	20.00	60.00	3.00	0.50	76.35	97.37	99.42
17	20.00	60.00	3.00	4.00	72.66	97.01	99.71
16	20.00	60.00	5.00	0.50	75.79	97.69	99.39
8	20.00	60.00	5.00	4.00	68.95	98.39	99.80
14	27.50	35.00	4.00	2.25	73.13	97.60	99.71
1	35.00	22.50	4.00	2.25	71.15	97.59	99.70
18	35.00	35.00	3.50	2.25	75.07	98.18	100.00
11	35.00	35.00	4.00	1.38	76.76	98.09	99.70
6	35.00	35.00	4.00	2.25	74.53	97.89	99.70
30	35.00	35.00	4.00	2.25	74.55	98.10	99.70
10	35.00	35.00	4.00	2.25	74.45	98.21	100.00
9	35.00	35.00	4.00	2.25	74.65	98.36	99.90
25	35.00	35.00	4.00	2.25	74.18	98.32	99.70
19	35.00	35.00	4.00	2.25	74.90	98.54	99.70
3	35.00	35.00	4.00	3.13	71.20	97.65	99.71
4	35.00	35.00	4.50	2.25	72.75	97.65	99.72
5	35.00	47.50	4.00	2.25	75.10	97.72	99.91
20	42.50	35.00	4.00	2.25	74.86	97.59	99.53
12	50.00	10.00	3.00	0.50	70.22	68.49	76.29
2	50.00	10.00	3.00	4.00	62.80	88.50	93.86
28	50.00	10.00	5.00	0.50	68.68	66.63	76.14
7	50.00	10.00	5.00	4.00	61.41	72.09	77.29
26	50.00	60.00	3.00	0.50	79.58	98.25	99.72
22	50.00	60.00	3.00	4.00	74.07	97.64	100.00
24	50.00	60.00	5.00	0.50	75.86	97.43	99.72
13	50.00	60.00	5.00	4.00	73.24	97.97	99.81

4.4 Analysis of Variance (ANOVA)

Adequacy and significance of quadratic model for each response, including COD, colour, and SS removal were tested by ANOVA, and results were represented in Table 4.5. F-test refers to a statistical test under null hypothesis that the mean of 3 or more groups is same. F-test of each model produced a very low p-value of < 0.0001 (p-value ≤ 0.05) in which indicated statistically significant, and sufficient evidence for rejection of null hypothesis (Gengec et al., 2011). All experiments are meaningless in case of all groups have same mean value. Meanwhile, significant lack of fit was represented by p-value of < 0.0001 for colour and SS, and 0.0032 for COD that lead to rejection of null hypothesis with no lack of linear fit. In the real world, there is no such a model fits perfectly without any occurrence of random and residual errors (Coleman and Vanatta, 2006). Random error is considered as pure error resulted by unpredictable changes in experiment. Residual error is deviation between actual response and predicted response for each data point, where both errors are partitioned in determination of inadequacy of the model (Coleman and Vanatta, 2006).

As presented in Table 4.6, goodness of fit on experimental data of COD, colour, and SS were verified by determination of coefficient (R^2) with values of 0.9881, 0.9612, and 0.9589 respectively. Higher R^2 values as close to 1 indicated each quadratic model was statistically desirable, better fit, and had reasonable agreement to experimental data (Asaithambi, Aziz and Daud, 2016; Bashir et al., 2016). In other words, a satisfactory agreement between experimental and predicted values was achieved (Tham, 2015). Predicted values of responses such as COD, colour, and SS removal were calculated accordingly through the following formulations as shown in Equation (4.1), (4.2), and (4.3). Operational variables such as current density, contact time, initial pH, and $S_2O_8^{2-}$ dosage were represented by X_1, X_2, X_3, and X_4. A good fit model should has at least $R^2 > 0.8$ (Myers et al., 2009). Furthermore, each quadratic model was also pointed with individual adjusted R^2 with values of 0.9828, 0.9464, and 0.9433. Irrelevant operational variables are added to model can lead to increase of R^2 and decrease of adjusted R^2. Hence, adjusted R^2 functions to "punish" who mindlessly involving extraneous variables and make

correction for inherent increase bias in R^2 (Dufour, 2011; Williams, 2015). On the other hand, predicted R^2 of each model with values of 0.9628, 0.9109, and 0.9025 depicted a reasonable agreement or range to adjusted R^2 respectively, and thus considered as acceptable model without possible problem between model and data (Setia, Kansal and Gayal, 2013). Model's favouritisms in this study were validated by adequate precision (AP) greater than 4 for COD, colour as well as SS with values of 52.369, 26.526, and 26.674 respectively (Bashir et al., 2016; Setia, Kansal and Gayal, 2013).

Dispersion of data points close to their respective expected values were highlighted by small standard deviation for COD, colour, and SS with values of 0.83, 3.28, and 2.88 respectively. In other words, experimental values were identified scattering around their respective predicted values, or evidence of insignificant variation for all models as shown in Figure 4.3 (Bashir et al., 2016).

Table 4.5 ANOVA for COD, Colour, and SS Removal

	Source	Sum of Square	*df	Mean Square	F value	p-value	Remarks
COD	Model	1135.30	9	126.14	185.24	< 0.0001	Significant
	Lack of Fit	13.34	15	0.89	15.91	0.0032	Significant
Colour	Model	5580.23	8	697.53	65.02	< 0.0001	Significant
	Lack of Fit	225.03	16	14.06	277.15	< 0.0001	Significant
SS	Model	4070.97	8	508.87	61.29	< 0.0001	Significant
	Lack of Fit	174.27	16	10.89	616.53	< 0.0001	Significant

*df – Degrees of freedom

Table 4.6 RSM Model Fit Summary

Statistical Figure	COD	Colour	SS
Standard Deviation	0.83	3.28	2.88
Coefficient of Variance (CV)	1.16	3.64	3.09
Predicted Residual Error Sum of Square (PRESS)	42.76	517.42	413.83
R^2	0.9881	0.9612	0.9589
Adjusted R^2	0.9828	0.9464	0.9433
Predicted R^2	0.9628	0.9109	0.9025
AP	52.369	26.526	26.674

$$\text{COD Removal} = 60.73381 + (0.16190 * X_1) + (0.64474 * X_2) - (0.91697 * X_3) - (1.00129 * X_4) - (0.002545 * X_1 * X_2) + (0.028929 * X_1 * X_4) + (0.029243 * X_2 * X_4) - (0.0055352 * X_2^2) - (0.69208 * X_4^2) \quad (4.1)$$

$$\text{Colour Removal} = 48.2415 + (0.43738 * X_1) + (2.27051 * X_2) - (5.56852 * X_3) + (3.24064 * X_4) - (0.00727 * X_1 * X_2) + (0.0962 * X_1 * X_3) - (0.054514 * X_2 * X_4) - (0.024413 * X_2^2) \quad (4.2)$$

$$\text{SS Removal} = 57.39929 + (0.45670 * X_1) + (1.90778 * X_2) - (5.41678 * X_3) + (3.07788 * X_4) - (0.00758833 * X_1 * X_2) + (0.091025 * X_1 * X_3) - (0.0507 * X_2 * X_4) - (0.02021 * X_2^2) \quad (4.3)$$

a)

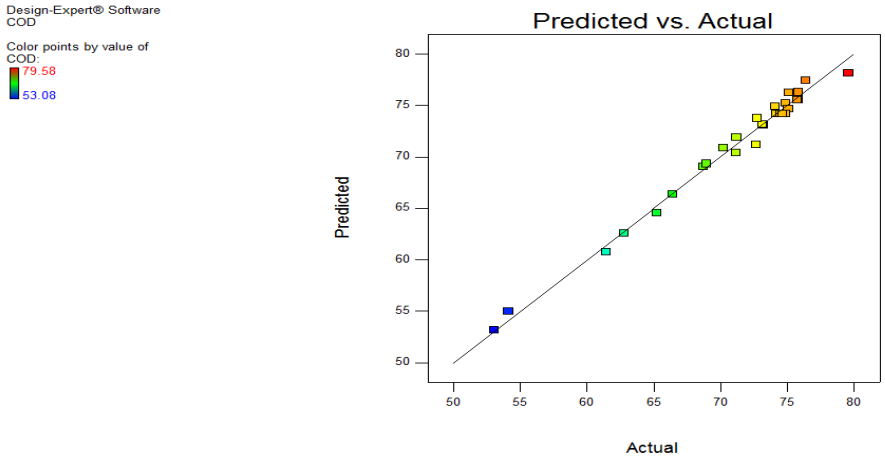

b)

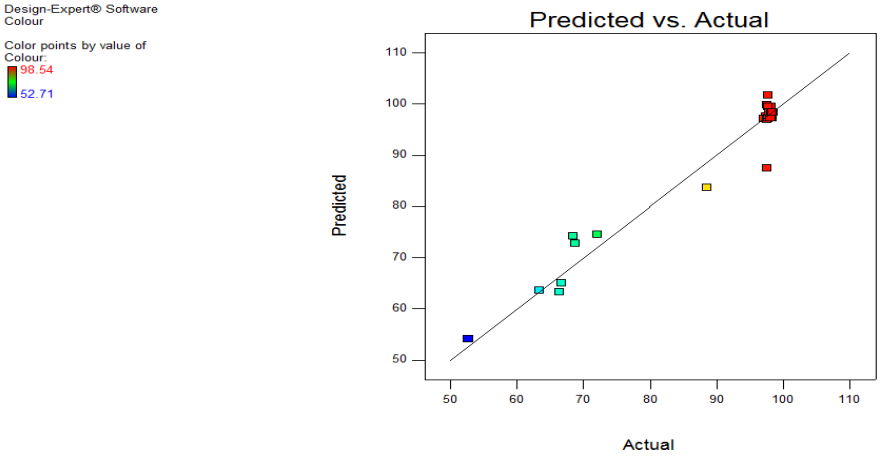

c)

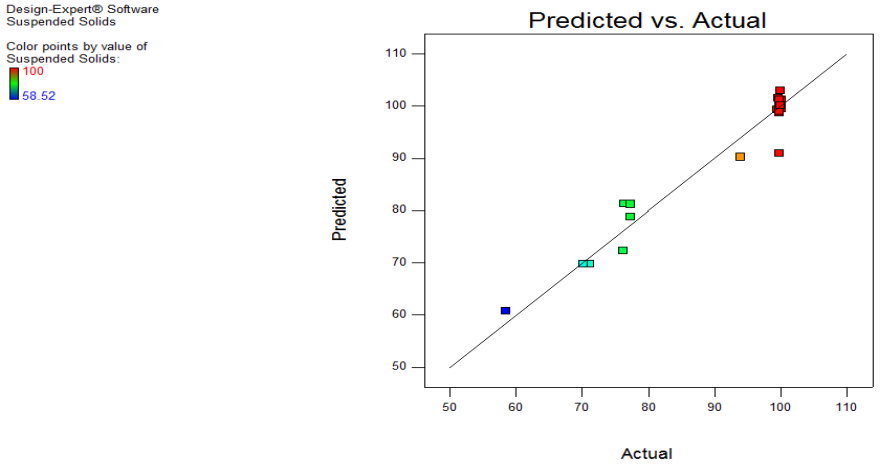

Figure 4.3 Correlation of Actual and Predicted Removal Efficiency of a) COD, b) Colour, c) SS

4.5 Experimental Analysis

Interactions between four operational variables and three responses were illustrated and described as below three-dimensional (3D) surface model graphs.

4.5.1 Effect of Operational Variables on COD

Current density and contact time were important operational conditions that had considerable effects on COD removal as shown in Figure 4.4 and 4.5. As expected, COD removal was increased when current density and contact time increased from 20 mA/cm^2 to 50 mA/cm^2 and 10 min to 60 min. This trend can be explained by more $MO_x(\cdot OH)$ formed at anode as well as $\cdot OH$ and $SO_4^{\cdot -}$ in bulk solution to simultaneously enhance organics degradation (Chen, Jhou and Huang, 2014; González-Vargas, Salazar and Sirés, 2014; Kariyajjanavar, Narayana and Nayaka, 2011).

Furthermore, different initial pH were adjusted accordingly in which affected the COD removal. As shown in Figure 4.4, a small decreasing trend was triggered when initial pH dropped from 3 to 5. Generally, mineralisation rate tends to be increased from alkaline to acidic condition (Bonyadinejad et al., 2015; Chen and Huang, 2015). Under acidic condition, H^+ are easily generated and act as catalyst to speed up $SO_4^{\cdot -}$ formation as shown in Equation (4.4) and (4.5) (Chia, 2016). At lower pH, formation of $MO_x(\cdot OH)$ at anode and $\cdot OH$ in the bulk solution are greatly improved due to minimisation of OER by increasing oxygen evolution over-potential value (Bonyadinejad et al., 2015). Besides, excessive formation of H_2O_2 as inhibitor of COD test is reduced under stronger acidic condition (Chen and Huang, 2015).

$$S_2O_8^{2-} + H^+ \rightarrow HS_2O_8^- \tag{4.4}$$

$$HS_2O_8^- \rightarrow H^+ + SO_4^{\cdot -} + SO_4^{2-} \tag{4.5}$$

Variation of $S_2O_8^{2-}$ dosages also represented as factor affecting COD removal. As shown in Figure 4.5, initial increasing $S_2O_8^{2-}$ dosage from 0.50 g to 1.38 g led to slightly increasing COD removal. This situation is revealed by increasing amount of $SO_4^{\cdot-}$ via cathodic reduction of $S_2O_8^{2-}$ that enhance organics degradation together with $\cdot OH$. However, after 1.38 g of $S_2O_8^{2-}$, there was a decrement of COD removal until 4.00 g of $S_2O_8^{2-}$. This is because too much of $S_2O_8^{2-}$ induce more H_2O_2 formation via hydrolysis of $S_2O_8^{2-}$ (Chen and Huang, 2015). Excessive H_2O_2 are susceptible to consume a portion of $Cr_2O_7^{2-}$ required in COD test to oxidise organics into CO_2 and H_2O as shown in Equation (4.6) (Talinli, 1992).

$$Cr_2O_7^{2-} + 3H_2O_2 + 8H^+ \rightarrow 2Cr^{3+} + 3O_2 + 7H_2O \qquad (4.6)$$

The highest removal efficiency of COD was 79.58 % with 50 mA/cm^2 of current density, 60 min of contact time, pH 3, and 0.50 g of $S_2O_8^{2-}$. In this case, 0.50 g of $S_2O_8^{2-}$ required highest performance requirements in order to get the highest removal, but normally existed in moderate removal. However, the second highest COD removal was 76.76 % that only required 35 mA/cm^2 of current density, 35 min of contact time, pH 4, and 1.38 g of $S_2O_8^{2-}$. The minimum COD removal was achieved at 53.08 % due to the lowest performance levels of current density and contact time, pH and $S_2O_8^{2-}$ dosage with values of 20 mA/cm^2, 10 min, pH 5, and 4.00 g of $S_2O_8^{2-}$ as shown in Table 4.3.

a)

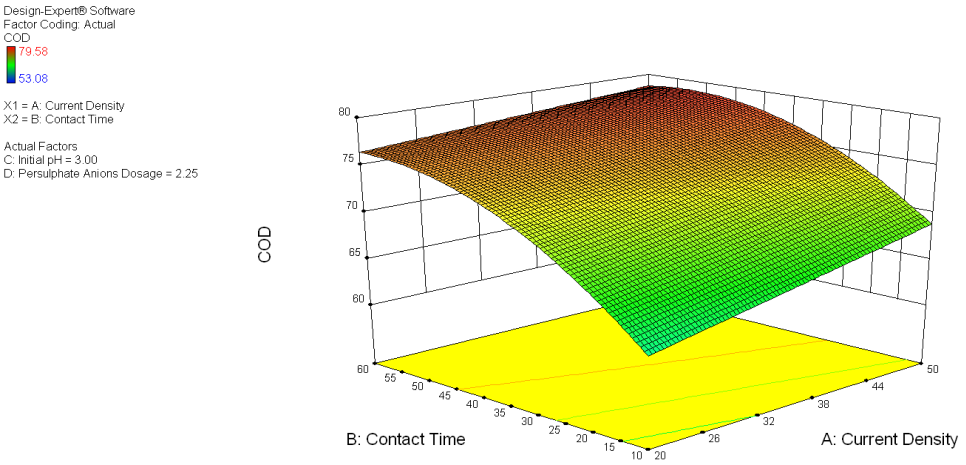

b)

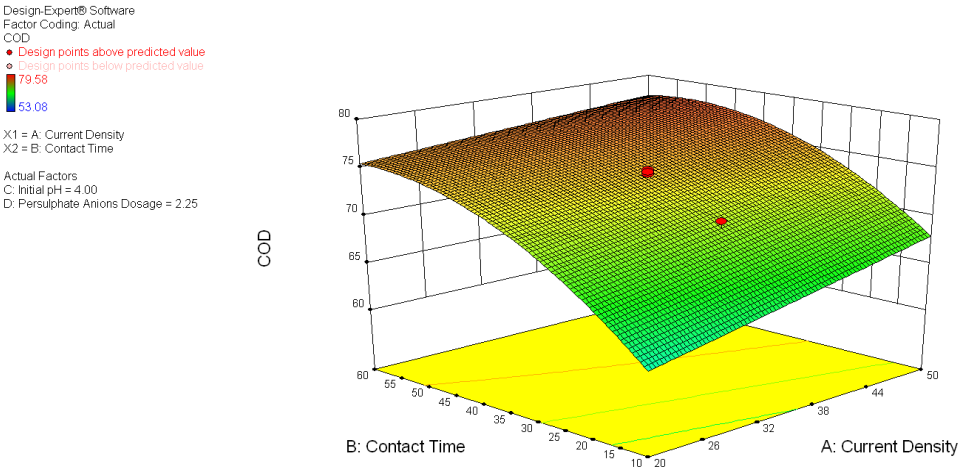

c)

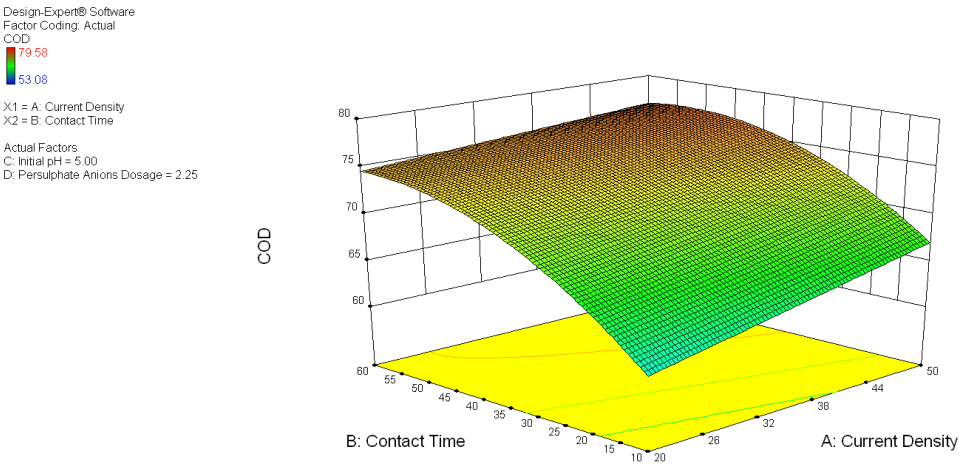

Figure 4.4 3D Surface Plot for COD Removal Efficiency a) pH 3 b) pH 4 c) pH 5

a)

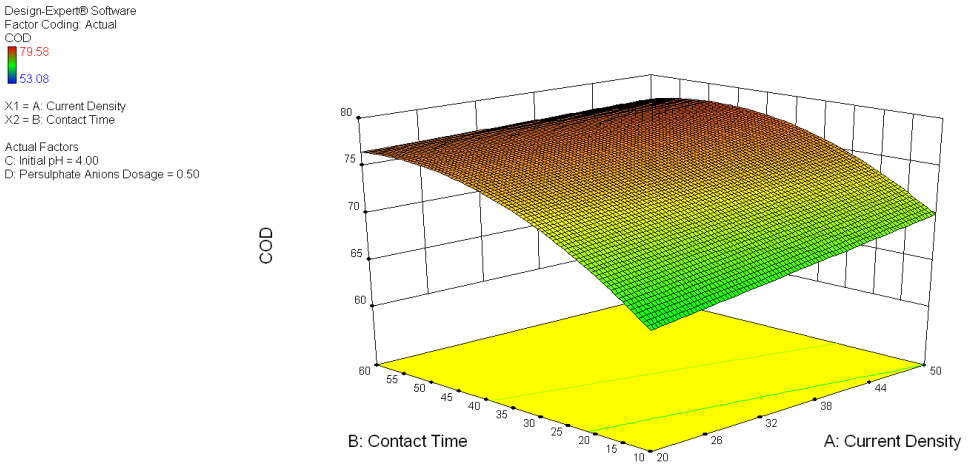

b)

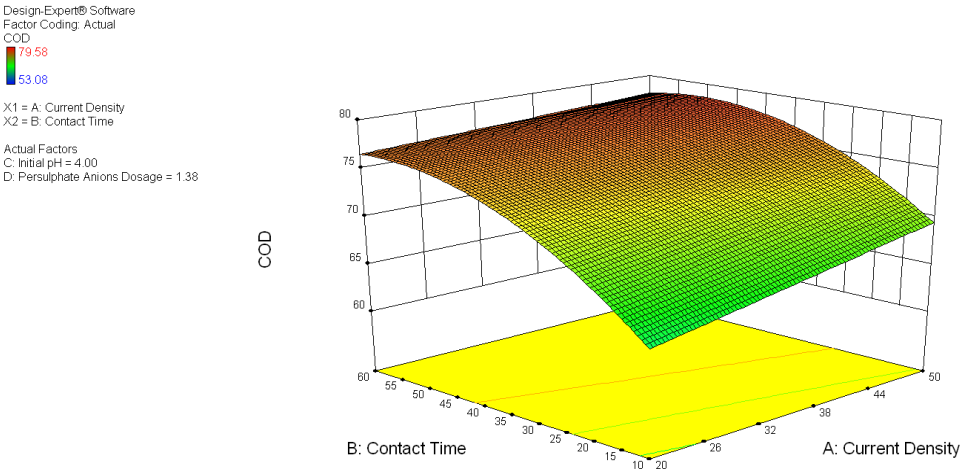

c)

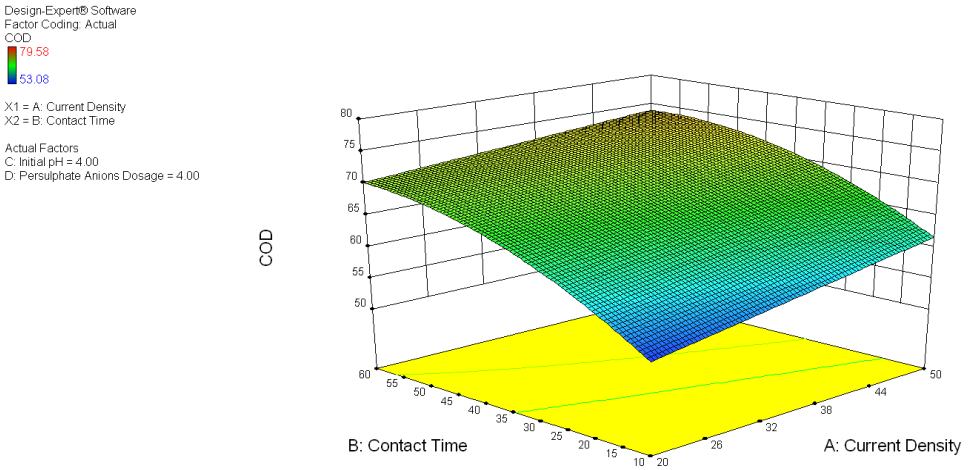

Figure 4.5 3D Surface Plot for COD Removal Efficiency a) 0.50 g b) 1.38 g c) 4.00 g of $S_2O_8^{2-}$

4.5.2 Effect of Operational Variables on Colour

Removal efficiency of colour was strongly affected by several operational variables, including current density, contact time, initial pH as well as $S_2O_8^{2-}$ dosage as shown in Figure 4.6 and 4.7. As predicted, increased current density and contact time from 20 mA/cm^2 to 50 mA/cm^2 and 10 min to 60 min could significantly increase removal efficiency of colour. As mentioned before, increasing both variables are able to generate numerous strong oxidising radicals either at anode or in bulk solution that operate simultaneously to boost up overall organics degradation (Chen, Jhou and Huang, 2014; González-Vargas, Salazar and Sirés, 2014; Kariyajjanavar, Narayana and Nayaka, 2011). However, colour removal only reached up to 97 % to 99 % after 22.5 min due to slow mineralisation rate was induced by reactions of remaining complex organic compounds as shown in Table 4.3 (Zhu, et al., 2014). On top of that, prolong contact time leads to high electrical energy consumption which is not preferable (Jumaah and Othman, 2015).

Furthermore, small decrement of colour removal was triggered by increasing initial pH from 3 to 5 as shown in Figure 4.6. This behaviour can be illustrated same as previous explanation of lower initial pH on COD removal in which more $MO_x(\cdot OH)$ and $\cdot OH$ form at anode and in bulk solution (Bonyadinejad et al., 2015). Meanwhile, more H^+ are generated in the solution which function as catalysts to initiate fast formation of $SO_4^{\cdot -}$ (Chia, 2016). Both phenomena illustrate organics mineralisation is enhanced by different oxidising radicals.

In addition, increasing $S_2O_8^{2-}$ dosage from 0.50 g to 4.00 g could had an small increasing trend on colour removal as shown in Figure 4.7. This situation is demonstrated by formation of more $SO_4^{\cdot -}$ with oxidation potential of 2.60 V via cathodic reduction of $S_2O_8^{2-}$. Under acidic condition, increasing amounts of H_2O_2 are also induced via hydrolysis of higher $S_2O_8^{2-}$ dosage, such as 1.38 g, 2.25 g, 3.13 g, and 4.00 g, where H_2O_2 are considered as oxidants with oxidation potential of 1.80 V (Abdullah, 2008; Chung et al., 2012). Besides, reduction of H_2O_2 at cathode is able to form powerful $\cdot OH$ with oxidation potential of 2.80 V as shown in

Equation (2.19) (Barrera-Díaz et al., 2014). Thus, combination of these radicals has ability to improve overall performance of electro persulphate oxidation.

The best possible colour removal was 98.54 % with conditions of 35 mA/cm^2 of current density, 35 min of contact time, pH 4, and 2.25 of $S_2O_8^{2-}$ dosage as shown in Table 4.3. However, the minimum colour removal was achieved at 52.71 % with the lowest performance conditions, including 20 mA/cm^2 of current density, 10 min of contact time, pH 5, and 0.50 of $S_2O_8^{2-}$ dosage.

a)

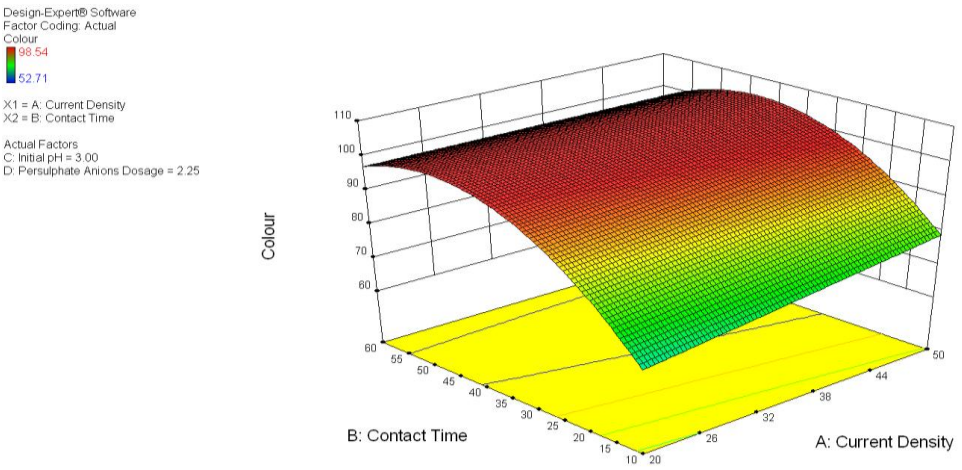

b)

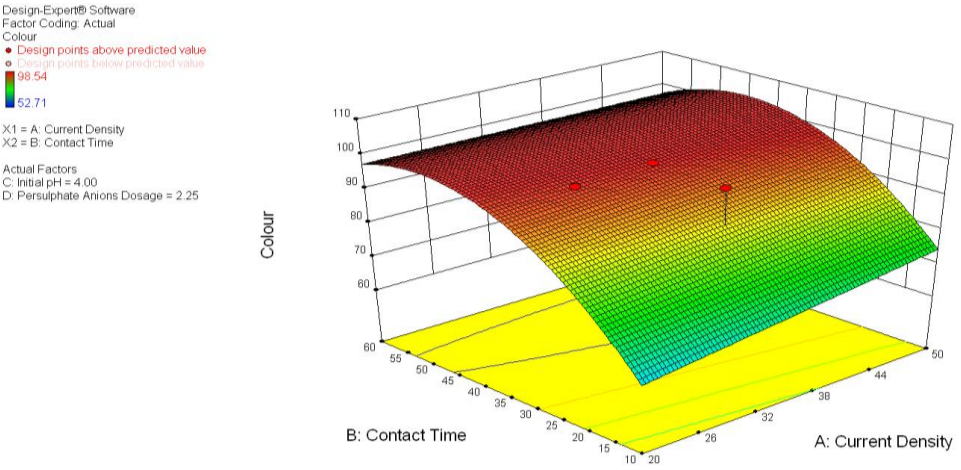

c)

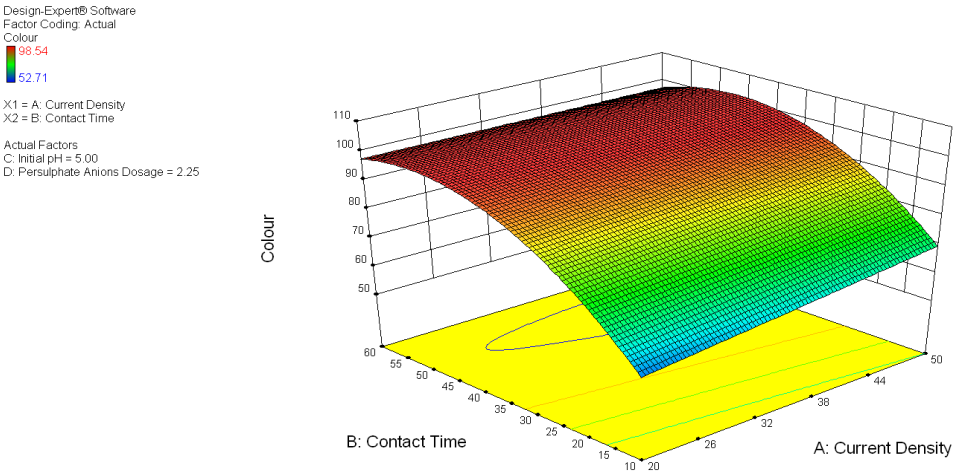

Figure 4.6 3D Surface Plot for Colour Removal Efficiency a) pH 3 b) pH 4 c) pH 5

a)

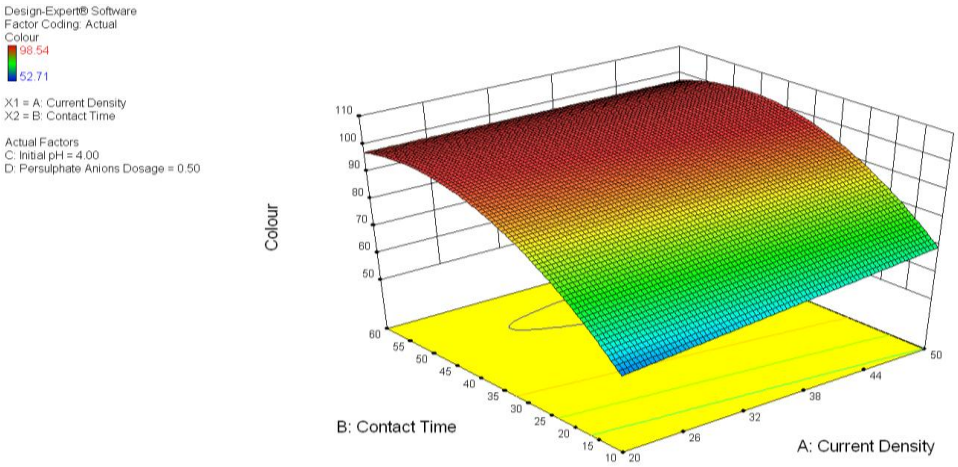

b)

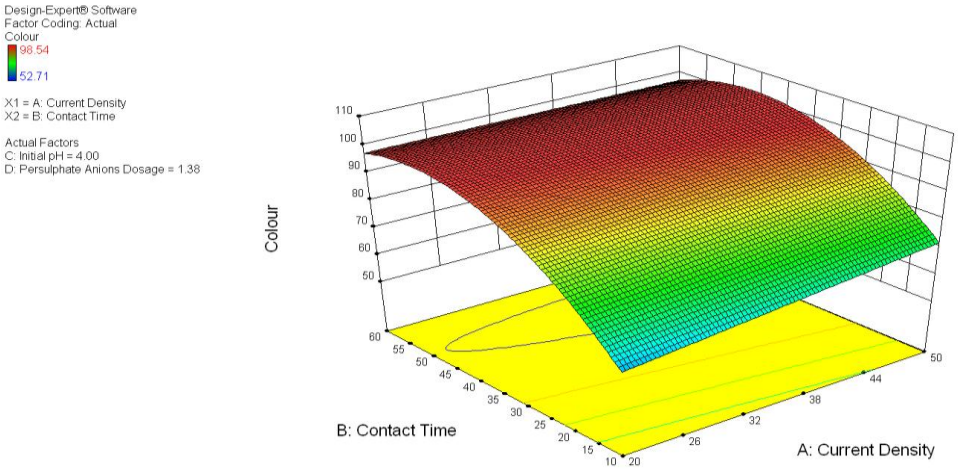

c)

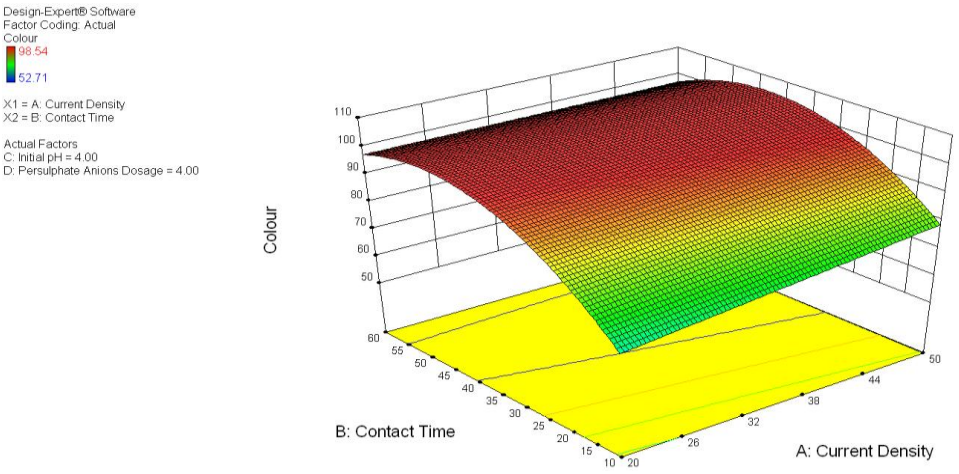

Figure 4.7 3D Surface Plot for Colour Removal Efficiency a) 0.50 g b) 1.38 g c) 4.00 g of $S_2O_8^{2-}$

4.5.3 Effect of Operational Variables on SS

SS removal was mainly dependent on electrocoagulation as well as electrofloatation. Performance of both processes was changed with several operational variables. According to Figure 4.8 and 4.9, current density and contact time played important roles in which increased both variables from 20 mA/cm^2 to 50 mA/cm^2 and 10 min to 60 min could contribute great SS removal. This case can be explained by Faraday's Law as amount of Al^{3+} generated at anode is increased by higher current density. Al^{3+} function as destabilising agents to encourage charge neutralisation of pollutants (Ozyonar and Karagozoglu, 2012; Ni'am et al., 2007; Rahmalan, 2009) Besides, increasing contact time promotes more Al^{3+} and OH^- at anode and cathode (Nasrullaha, Singh and Wahid, 2012). Both phenomena introduce high $Al(OH)_3$ formation in solution. $Al(OH)_3$ have high adsorption properties to bond with destabilised pollutants, and form large lattice-structures or flocs (Kabdaşlı et al., 2012). Furthermore, increasing current density leads to increasing production rate of H_2 bubbles and decreasing size of bubbles (Ozyonar and Karagozoglu, 2012). High surface area per unit volume of gas is provided by small bubbles in order to allow more trapped pollutants or large flocs to attach (Mickova, 2015). Eventually, large flocs can be removed from aqueous medium either through sedimentation or H_2 bubbles floatation (Jotin, Ibrahim and Halimoon, 2012).

$Al(OH)_3$ are predominant aluminium chemical species at pH 4 to 9.5, and thus lead to more effective treatment (Jotin, Ibrahim and Halimoon, 2012). Actually, SS removal at pH 5 should greater than pH 4 followed pH 3. However, pH 3 to 5 induced a small decreasing trend for SS removal as shown in Figure 4.8. This is because $SO_4^{\cdot -}$ are predominant at lower pH which allow fast rate organics degradation (Chia, 2016). Also, electrocoagulation has a capability to physically remove organics via sweep coagulation (Askari et al., 2014). Thus, majority of organics are degraded in short interval, resulting less competition occurs between organics and SS to be destabilised and bonded with $Al(OH)_3$. Moreover, fast formation of H_2 bubbles takes place at lower pH, and smallest bubbles are formed at pH 3 to 4 with approximate 16 μm in diameter (Mickova, 2015; Moreno et al., 2007). Again, small bubbles provide more surface areas for trapped pollutants to attach and

float to top surface. All Above situations could be observed in Table 4.3 with same conditions of 20 mA/cm^2 of current density, 10 min of contact time, 0.50 g of $S_2O_8^{2-}$, only different in pH 3 and 5.

According to Figure 4.9, $S_2O_8^{2-}$ dosage increased from 0.50 g to 4.00 g resulted in small increment of SS removal. As mentioned before, higher $S_2O_8^{2-}$ dosage induces more formation of $SO_4^{\cdot-}$ via reduction of $S_2O_8^{2-}$ at cathode, and enhance organics degradation together with $\cdot OH$ in order to encourage less competition with SS. Therefore, SS have more chances to be destabilised and bonded by $Al(OH)_3$, eventually are removed out from the aqueous medium.

The best SS removal was 100 % with conditions of 35 mA/cm^2 of current density, 35 min of contact time, pH 4, and 2.25 of $S_2O_8^{2-}$ dosage as shown in Table 4.3. However, the minimum of SS removal was achieved at 58.52 % with lowest performance conditions, including 20 mA/cm^2 of current density, 10 min of contact time, pH 5, and 0.50 of $S_2O_8^{2-}$ dosage. Normally, contact time more than 22.5 min was able to achieve 99 % to 100 % of SS removal. However, prolong contact time may induce higher electrical energy consumption which is not preferable in economic consideration.

a)

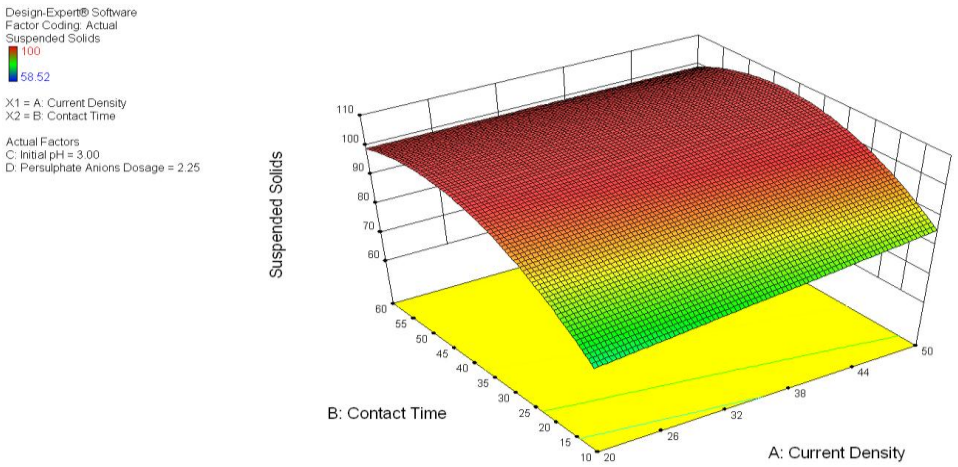

b)

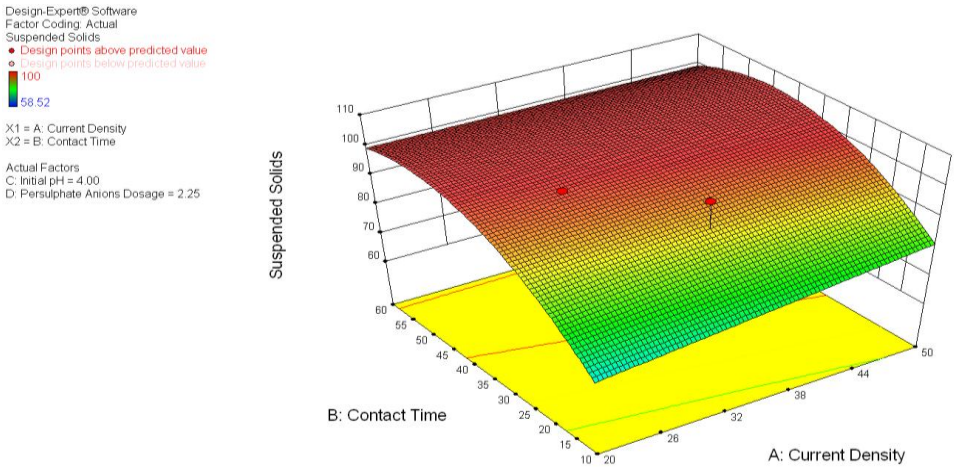

c)

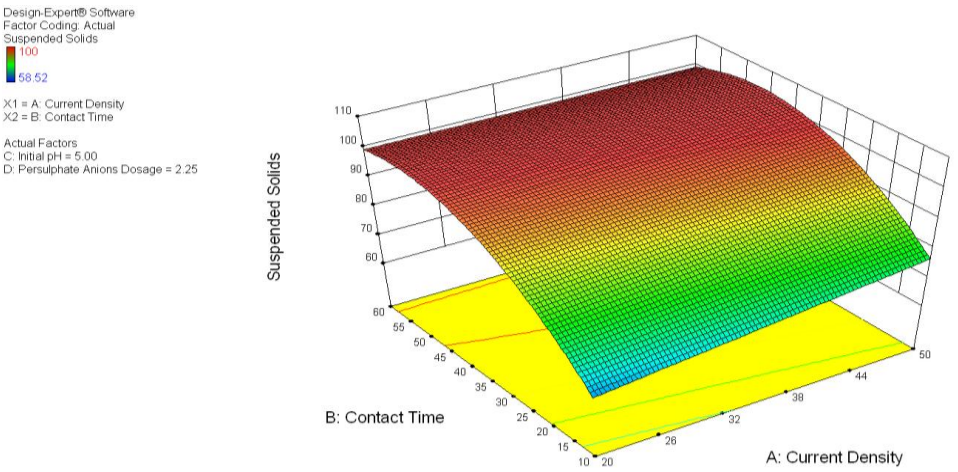

Figure 4.8 3D Surface Plot for SS Removal Efficiency a) pH 3 b) pH 4 c) pH 5

a)

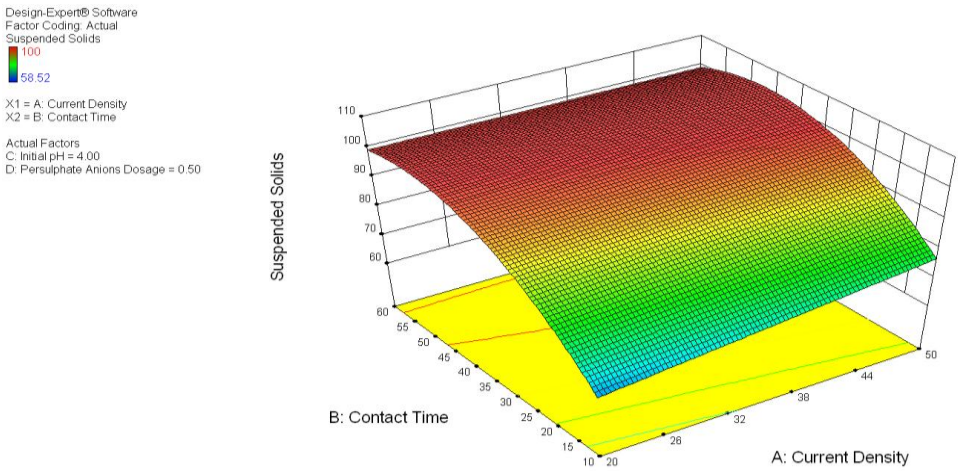

b)

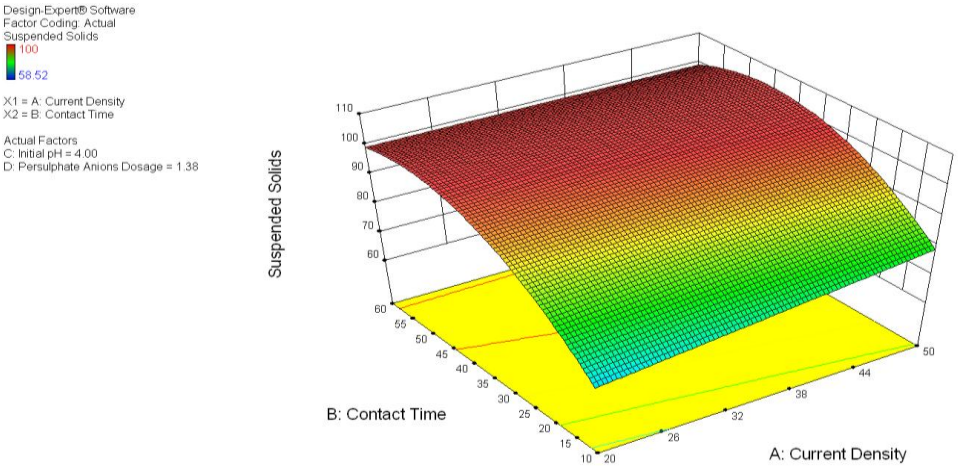

c)

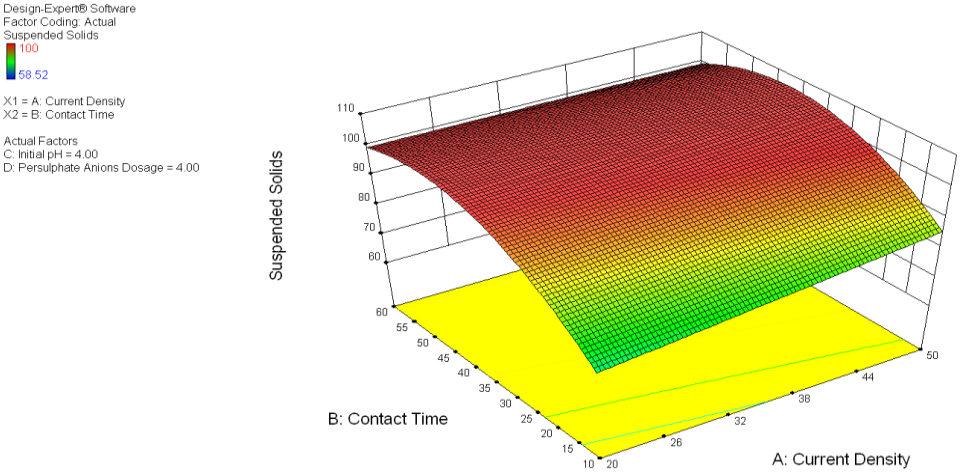

Figure 4.9 3D Surface Plot for SS Removal Efficiency a) 0.50 g b) 1.38 g c) 4.00 g of $S_2O_8^{2-}$

4.6 Optimisation

One of the main objectives of this research is to acquire optimum operational conditions in order to get promising performance of COD, colour, and SS removal. All experimental results were optimised by using regression equations of RSM in DOE. Through optimisation, optimum operational variables were selected within respective range, including 45 mA/cm^2 of current density, 45 min of contact time, pH 4, and 0.892 g of $S_2O_8^{2-}$. This set of variables was selected based on desirability with value of 0.978 that indicated predicted responses were almost close to target requirements (Khor, Jaafar and Ramakrishnan, 2016). Desirability of 1 was unable to achieve due to minor adjustment at lower and upper limit of range of operational variables before optimisation, such as 20 to 45 mA/cm^2 of current density, 10 to 45 min of contact time, pH 3 to 4, and 0.50 to 1.50 g of $S_2O_8^{2-}$. Minor adjustment was crucial in economic consideration in which increased process efficiency by reducing electrical energy, time, and chemical dosage consumption, while provided promising removal efficiency. Besides, a set of experiment with optimum operational conditions was carried out for confirmation of actual and predicted experimental data as shown in Table 4.7.

Table 4.7 Optimisation and Laboratory Experiment Validation (45 mA/cm^2 of Current Density, 45 min of Contact Time, pH 4, and 0.892 g of $S_2O_8^{2-}$)

Response	Predicted Removal Efficiencies,%	Actual Removal Efficiencies, %
COD	77.87	77.70
Colour	100.00	97.96
SS	100.00	99.72

As shown in Table 4.7, actual and predicted removal efficiencies had slightly different because of human and random errors that indirectly affected end results. For COD removal, actual value of 77.70 % was very close to predicted value of 77.87 % that indicated the lowest errors occurred in experimental work. Moreover, colour removal had achieved up to 97.96 % and as for the predicted value, it should be treated up to 100 %. Last but not least, SS removal had provided a promising

performance in which achieved close to 100 % with a final removal efficiency of 99.72 %. Overall actual data for each respective response stilled achieve within desirable treatment efficiency, and thus optimum operational conditions were accepted.

A summary of treatment efficiencies for several heavy metals such as Al, Cr, Fe, Ni, Pb, and Zn as well as $NH_3 - N$ by electro persulphate oxidation were shown in Table 4.8. Inductively Coupled Plasma-Mass Spectrophotometer (ICP-MS) was employed to determine initial and final concentration of heavy metals present in biologically treated POME, and thus removal efficiency could be calculated respectively. Generally, heavy metals in aqueous medium are removed through electrocoagulation as $Al(OH)_3$ act as adsorbents for M^{n+}. Also, M^{n+} can react with OH^- to form corresponding hydroxides, and eventually settle down which is known as co-precipitation (Bazrafshan et al., 2008). Through ICP-MS, trace amounts of Cr, Ni, and Pb were found in untreated sample. However, treated sample stilled remain small amounts with values of 1.979 ppb, 0.385 ppb, and 0.455 ppb. This situation can be explained by not all of these heavy metals are existed in M^{n+}, so less precipitation occurs. Also, Fe and Zn were detected to had moderate removal efficiencies via electro persulphate oxidation from 101.881 ppb and 51.281 ppb to 77.584 ppb and 23.731 ppb. However, final concentration of Al, 12.050 ppb seemed to be higher than initial concentration of 10.695 ppb due to anodic dissolution of aluminium plate that increased amounts of Al^{3+} in treated sample. Other than heavy metals, $NH_3 - N$ in untreated and treated sample were also tested, where only 9.09% of removal efficiency was achieved. Actually, initial concentration of $NH_3 - N$ was not that high only with 55 mg/L, and already fulfilled within discharge limit of 150 mg/L (Lorestani, 2006; Shahrifun, et al., 2015). Therefore, $NH_3 - N$ was not a main factor to be investigated in this study, but tested for better understanding. After the electro persulphate oxidation, colour and turbidity between untreated and treated sample were obviously different as shown in Figure 4.10. Table 4.9 shows the comparison between treated sample and regulatory discharge standards of POME according to EQA 1974.

Table 4.8 Treatment Efficiencies of Heavy Metals and $NH_3 - N$ by Using Electro Persulphate Oxidation

*Parameter	Initial	Final	Removal Efficiencies, %
Al	10.695	12.050	-12.67
Cr	3.015	1.979	34.36
Fe	101.881	77.584	23.85
Ni	1.263	0.385	69.52
Zn	51.281	23.731	53.72
Pb	0.551	0.455	17.42
$NH_3 - N$	55	50	9.09

*All parameters are expressed in ppb, except $NH_3 - N$ (mg/L).

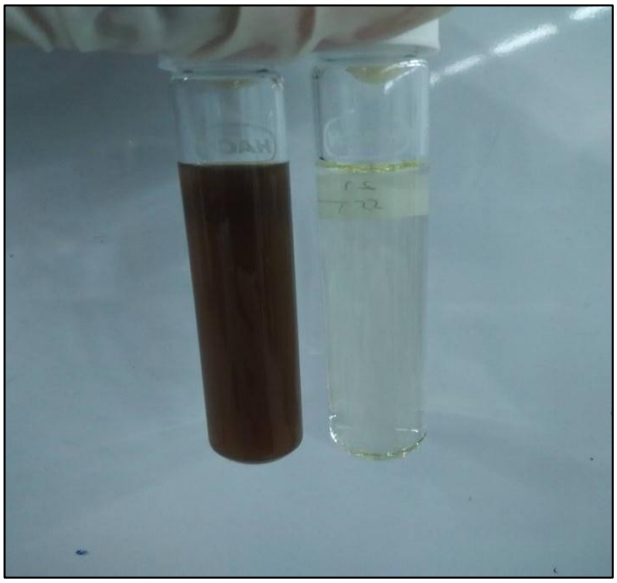

Figure 4.10 Comparison between Untreated (Left) and Treated (Right) Sample After the Electro Persulphate Oxidation

Table 4.9 Treated Sample Versus Regulatory Discharge Standards of POME According to EQA 1974 (Lorestani, 2006; Shahrifun, et al., 2015)

*Parameter	Initial	Final	Removal Efficiencies, %	Regulatory Discharge Standards
COD	2510	560	77.70	1000
Colour	5380	110	97.96	-
SS	353	1	99.72	400
pH	4.01	5.88	-	5 - 9
$NH_3 - N$	55	50	9.09	150

*All parameters are expressed in mg/L, except colour ($PtCo$) and pH.

4.7 Cost Estimation

Cost of electrical energy consumption was determined based on literature, where all calculation steps were shown below (Bashir et al., 2016). Besides, calculation of cost of $Na_2S_2O_8$ required in electro persulphate oxidation was also shown below.

Electrical Energy Consumption = Current Density × Anode Surface Area × Voltage × Contact Time × $(\frac{1000\ L}{Sample\ Volume})$

$= 45 \times 27 \times 12 \times \frac{45}{60} \times \frac{1000}{0.5} \times 10^{-6}$

$= 21.87\ kWh/m^3$

Cost of Electrical Energy Consumption = $21.87\ kWh/m^3 \times 0.218\ MYR/kWh$

$= 4.77\ MYR/m^3$

Cost of $Na_2S_2O_8$ = 350 $USD/metric\ tonne$ × 4.09 MYR/USD

= 1431.50 $MYR/metric\ tonne$

= 1.43 MYR/kg (1 $metric\ tonne$ = 1000 kg)

Each set of experiment required 1.128 g of $Na_2S_2O_8$, where 1 kg of $Na_2S_2O_8$ could treat about 887 times of 500 ml of biologically treated POME or equal to 0.4435 m^3. Therefore, treating each cubic meter of biologically treated POME needed 3.22 MYR.

CHAPTER 5

CONCLUSION AND RECOMMENDATIONS

5.1 Conclusion

In this study, a series of 30 experiments were conducted and R^2 with values of 0.9881, 0.9612, and 0.9589 were obtained close to 1. This situation indicated each quadratic model such as COD, colour, and SS removal was statistically desirable, better fit, and had reasonable agreement to experimental data. Current density and contact time considered as the main factors affecting electro persulpahte oxidation as compared to initial pH and $S_2O_8^{2-}$ dosage which had more significant effects. Besides, optimum operational conditions for electro persulphate oxidation to treat biologically treated POME, such as current density, contact time, initial pH, and $S_2O_8^{2-}$ dosage were experimentally determined as 45 mA/cm^2, 45 min, pH 4, and 0.892 g respectively. Results obtained from optimised conditions with values of 77.70 % removal for COD, 97.96 % removal for colour, and 99.72 % removal for SS were further compared to regulatory discharge standards of POME, where tested parameters such as COD and SS fulfilled requirements decreed by EQA 1974 with values less than 1000 mg/L and 400 mg/L. Furthermore, synergistic effect of $S_2O_8^{2-}$ on electrooxidation had significantly improved process efficiencies and maintained promising removal efficiencies as compared to electrooxidation alone. According to previous study, 69.56 % of COD removal and 97.80 % of colour removal required optimum operational conditions with values of 56 mA/cm^2 of current density, 65 min of contact time, and pH 4.5 (Tham, 2015). Upon these findings, electro persulphate oxidation was proven as a suitable post treatment of

biologically treated POME. Also, overall treatment cost could be reduced through less consumption of electrical energy and contact time. For the electro persulphate oxidation, treating each cubic meter of biologically treated POME only required 4.77 MYR that was cheaper than electrooxidation that required 8.56 MYR (Bashir et al., 2016). On top of that, cost of $Na_2S_2O_8$ required in the electro persulphate oxidation was considered reasonable as treating each cubic meter of biologically treated POME only required 3.22 MYR.

5.2 Recommendations for Future Research

Through this research, several recommendations should be suggested in order to investigate other possibilities to further enhance treatment efficiencies as well as fulfill all stringent regulations. First, selecting other types of electrodes like non-active anodes, including lead dioxide (PbO_2) and antimony-doped tin oxide ($SnO_2 - Sb_2O_5$) that have higher oxygen evolution overpotential. Also, these electrodes act as poor electro-catalysts for OER, where encourage complete oxidation of organics, and thus providing an effective process (Martínez-Huitle and Andrade, 2011). Besides, other alternative energy sources can be selected to replace demand of electrical energy from DC power supply, such as biogas or sunlight. Last but not least, other operational conditions such as agitation speed as well as distance between electrodes have potential to be further studied in future. Since interaction between pollutants and oxidants or coagulants becomes weak when distance is increased. On top of that, adequate agitation speed is able to ensure both oxidants and coagulants completely disperse in solution which can promote excellent homogenisation (Naje et al., 2015).

REFERENCES

Abdullah, N. and Sulaiman, F., 2013. The oil palm wastes in Malaysia. In: M.D. Matovic, ed. *Biomass now-sustainable growth and use*. Croatia: Intech. pp. 75-100.

Abdullah, S.B., 2008. *Tertiary treatment of palm oil mill effluent (POME) using hydrogen peroxide photolysis method*. Postgraduate. Universiti Teknologi Malaysia.

Abdurahman, N.H., Azhari, N.H. and Rosli, Y.M., 2013. Ultrasonic membrane anaerobic system (UMAS) for palm oil mill effluent (POME) treatment. In: N.W.T. Quinn, ed. *International perspectives on water quality management and pollutant control*. Croatia: Intech. pp. 108-120.

Abu Amr, S.S., Aziz, H.A. and Adlan, M.N., 2013. Optimization of stabilized leachate treatment using ozone/persulfate in the advanced oxidation process. *Waste Management*, 33(6), pp. 1434-1441.

Ahmed, M.M., 2008. Electrochemical oxidation of acid yellow and acid violet dyes assisted by transition metal modified kaolin. *Portugaliae Electrochimica Acta*, 26(6), pp. 547-557.

Al-Hashimi, M.A.I. and Hussain, H.T., 2013. Stabilization pond for wastewater treatment. *European Scientific Journal*, 9(14), pp. 278-294.

Ali, E. and Yaakob, Z., 2012. Electrocoagulation for treatment of industrial effluents and hydrogen production. In: V. Linkov, ed. *Electrolysis*. Croatia: Intech. pp. 227-242.

Ameta, R., Kumar, A., Punjabi, P.B. and Ameta, S.C., 2012. Advanced oxidation processes: Basics and Applications. In: D.G. Rao, R. Senthikumar, J. Anthony Byrne and S. Feroz, eds. *Wastewater treatment advanced processes and technologies*. Boca Raton: CRC Press, pp. 61-63.

Aris, A., Ooi, B.W., Kon, S.K. and Ujang, Z., 2008. Tertiary treatment of palm oil mill effluent using fenton oxidation. *Malaysian Journal of Civil Engineering*, 20(1), pp. 12-25.

Asaithambi, P., Aziz, A.R.A. and Daud, W.M.A.B.W., 2016. Integrated ozone-electrocoagulation process for the removal of pollutant from industrial effluent: optimization through response surface methodology. *Chemical Engineering and Processing*, 105(2016), pp. 92-102.

Askari, M., Alimohammadi, M., Dehghani, M.H., Emamjomeh, M.M. and Nazmara, S., 2014. Removal of natural organic matter from aqueous solutions by electrocoagulation. *J Adv Environ Health Res*, 2(2), pp. 91-100.

Azoddein, A.A.M., Haris, H.B. and Azli, F.A.M., 2015. Treatment of palm oil mill effluent (POME) using membrane bioreactor. *Malaysian Journal of Analytical Sciences*, 19(3), pp. 463-471.

Badroldin, N.A.B., 2010. *Treatment of palm oil mill effluent (POME) using hybrid up flow anaerobic sludge blanket (HUASB) reactor*. Postgraduate. Universiti Tun Hussein Onn Malaysia.

Bala, J.D., Lalung, J. and Ismail, N., 2014. Biodegradation of palm oil mill effluent (POME) by bacterial. *International Journal of Scientific and Research Publications*, 4(3), pp. 1-10.

Barrera-Díaz, C., Cañizares, P., Fernández, F.J., Natividad, R. and Rodrigo, M.A., 2014. Electrochemical advanced oxidation processes: an overview of the current applications to actual industrial effluents. *J. Mex. Chem. Soc*, 58(3), pp. 256-275.

Bashir, M.J.K., Tham, M.H., Lim, J.W., Ng, C.A. and Abu Amr, S.S., 2016. Polishing of treated palm oil mill effluent (POME) from ponding system by electrocoagulation process. *Water, Science & Technology*, 74(3), pp. 2704-2712.

Bashir, M.J.K., Abu Amr, S.S., Aziz, S.Q., Ng, C.A. and Sethupathi, S., 2015. Wastewater treatment processes optimization using response surface methodology (RSM) compared with conventional methods: review and comparative study. *Middle-East Journal of Scientific Research*, 23(2), pp. 244-252.

Bazrafshan, E., 2008. Performance evaluation of electrocoagulation process for removal of chromium (VI) from synthetic chromium solutions using iron and aluminum electrodes. *Turkish J. Eng. Env. Sci.*, 32 (2), pp. 59-66.

Bello, M.M., Nourouzi, M.M. and Abdullah, L.C., 2014. Tertiary treatment of biologically treated POME in fixed-bedC: color and COD removal. *Advances in Environmental Biology*, 8(3), pp. 565-571.

Bonyadinejad, G., Khosravi, M., Ebrahimi, A., Nateghi, R., Taghavi-Shahri, S.M. and Mohammadi, H., 2015. Sonoelectrochemical mineralization of perfluorooctanoic acid using Ti/PbO_2 anode assessed by response surface methodology. *Journal of Environmental Health Science & Engineering*, 13(1), pp. 1-9.

Bornare, J.B., Raman, V.K., Sapkal, V.S., Sapkal, R.S., Minde, G. and Sapkal, P.V., 2014. An overview of membrane bioreactors for anaerobic treatment of wastewaters. *International Journal of Innovative Research in Advanced Engineering (IJIRAE)*, 1(7), pp. 91-97.

Bradley, N., 2007. *The response surface methodology*. Postgraduate. Indiana University of South Bend.

Britto-Costa, P.H. and Ruotolo, L.A.M., 2012. Phenol removal from wastewater by electrochemical oxidation using boron doped diamond (BDD) and $Ti/Ti_{0.7}Ru_{0.3}O_2$ DSA® electrodes. *Brazilian Journal of Chemical Engineering*, 29(4), pp. 763-773.

Calabria, A. and Capata, R., 2012. Power generation with vegetable oils in the Italian scenario: a 20 MW case study. Technical feasibility analysis and economical aspects. *Engineering*, 4(9), pp. 548-556.

Chen, W.S. and Huang, C.P., 2015. Mineralization of aniline in aqueous solution by electrochemical activation of persulfate. *Chemosphere*, 125 (2015), pp. 175-181.

Chen, W.S., Jhou, Y.C. and Huang, C.P., 2014. Mineralization of dinitrotoluenes in industrial wastewater by electro-activated persulfate oxidation. *Chemical Engineering Journal*, 252 (2014), pp. 166–172.

Chia, K.L., 2016. *Persulphate oxidation of palm oil mill effluent (POME): post treatment process*. Uundergraduate. Universiti Tunku Abdul Rahman.

Chong, S.H., Sen, T.K., Kayaalp, A. and Ang, H.M., 2012. The performance enhancements of upflow anaerobic sludge blanket (UASB) reactors for domestic sludge treatment - a state-of-the-art review. *Water Research*, 46(11), pp. 3434-3470.

Chung, T.V., Ket, NG.D., Bay, D.V., Luong, T.D. and Huong, NG.TH., 2012. Degradation of 2,4,6-trinitroresorcinol by persulfate oxidation. *Asian Journal of Chemistry*, 24(1), pp. 437-440.

Coleman, D. and Vanatta, L., 2006. *Statistics in analytical chemistry: part 22-lack-of-fit details*. [online] Available at: <http://www.americanlaboratory.com/913-Technical-Articles/1238-Part-22-Lack-of-Fit-Details/> [Accessed 25 July 2016].

Cronk, G., 2008. Cronk, Gary. Case study comparison of multiple activation methods for sodium persulfate ISCO treatment. In: Battelle, *Sixth International Conference on Remediation of Chlorinated and Recalcitrant Compounds*. Monterey Conference Center, 19 - 22 May, 2008. US: JAG Consulting Group.

Doosti, M.R., Kargar, R. and Sayadi, M.H., 2012. Water treatment using ultrasonic assistance: a review. *Proceedings of the International Academy of Ecology and Environmental Sciences*, 2(2), pp. 96-110.

Dufour, J.M., 2011. *Coefficients of determination*. [online] Available at: < http://www2.cirano.qc.ca/~dufourj/Web_Site/ResE/Dufour_1983_R2_W.pdf> [Accessed 28 July 2016].

Fadzil, N.A.M., Zainal, Z. and Abdullah, A.H., 2013. COD removal for palm oil mill secondary effluent by using UV/Ferrioxalate/ TiO_2 / O_3 system. *International Journal of Emerging Technology and Advanced Engineering*, 3(7), pp. 237-243.

Feng, Z., Feng, C.P., Li, W.Q. and Cui, J.G., 2014. Indirect electrochemical oxidation of dye wastewater containing acid orange 7 using Ti / RuO_2 - Pt electrode. *International Journal of Electrochemical Science*, 9 (2), pp. 943-954.

Frederickson, K.C., 2005. *The application of a membrane bioreactor for wastewater treatment on a Northern Manitoban aboriginal community*. Postgraduate. University of Manitoba Winnipeg.

Gan, P.Y. and Li, Z.D., 2014. Econometric study on Malaysia's palm oil position in the world market to 2035. *Renewable and Sustainable Energy Reviews*, 39(2014), pp. 740-747.

Gengec, E., Kobya, M., Demirbas, E., Akyol, A. and Oktor, K., 2012. Optimization of baker's yeast wastewater using response surface methodology by electrocoagulation. *Desalination*, 286(2012), pp. 200-209.

Gomathi, V.C., Ramanathan, B., Nallapeta, A.S., Ramanjaneya, V., Mula, R. and Jayasimha Rayalu, D., 2012. Decolourization of paper mill effluent by immobilized cells of phanerochaete chrysosporium. *International Journal of Plant, Animal and Environmental Sciences*, 2(1), pp. 141-146.

González-Vargas, C., Salazar, R. and Sirés, I., 2014. Electrochemical treatment of acid red 1 by electro-fenton and photoelectro-fenton processes. *J. Electrochem. Sci. Eng.*, 4(4), pp. 235-245.

Hassan, S., Kee, L.S. and Al-Kayiem, H.H., 2013. Experimental study of palm oil mill effluent and oil palm frond waste mixture as an alternative biomass fuel. *Journal of Engineering Science and Technology*, 8(6), pp. 703-712.

Hu, J.M., 2013. *Anaerobic digestion of sludge from brackish RAS: CSTR performance, analysis of methane potential and phosphatase, struvite crystallization*. Postgraduate. Delft University of Technology.

Idris, M.A., Jami, M.S. and Muyibi, S.A., 2010. Tertiary treatment of biologically treated palm oil mill effluent (POME) using UF membrane system: effect of MWCO and transmembrane pressure. *International Journal of Chemical and Environmental Engineering*, 1(2), pp. 108-112.

Igwe, J.C. and Onyegbado, C.C., 2007. A review of palm oil mill effluent (POME) water treatment. *Global Journal of Environmental Research*, 1(2), pp. 54-62

Jones-Lee, A. and Lee, G.F., 2005. Eutrophication (excessive fertilization). In: J.H. Lehr and J. Keeley, eds. *Water encyclopedia*. Hoboken: John Wiley & Sons, Inc. pp. 107-114.

Jotin, R., Ibrahim, S. and Halimoon, N., 2012. Electro coagulation for removal of chemical oxygen demand in sanitary landfill leachate. *International Journal of Environmental Sciences*, 3(2), pp. 921-930.

Jumaah, M.A. and Othman, M.R., 2015. COD removal from landfill leachate by electrochemical method using charcoal-PVC electrode. *International Journal of ChemTech Research*, 8(12), pp. 604-609.

Kabdaşlı, I., Arslan-Alaton, I., Ölmez-Hancı, T. and Tünay, O., 2012. Electrocoagulation applications for industrial wastewaters: a critical review. *Environmental Technology Reviews*, 1(1), pp. 2-45.

Kandasamy, J., Vigneswaran, S. and Hoang, T.T.L., 2009. *Adsorption and biological filtration in wastewater treatment*. 1st ed. Singapore: Encyclopedia of Life Support Systems (EOLSS).

Kapalka, A., 2008. *Reactivity of electrogenerated free hydroxyl radicals and activation of dioxygen on boron-doped diamond electrodes*. PhD. AGH University of science and technology.

Kariyajjanavar, P., Narayana, J. and Nayaka, Y.A., 2011. Degradation of textile wastewater by electrochemical method. *Hydrol Current Res*, 2(1), pp. 1-7.

Khalid, S., 2011. *Studies on development of new methodologies for analysis and treatment of aromatic sulphonates in aquatic environment*. PhD. Jawaharlal Nehru Technological University.

Khandegar, V. and Saroha, A.K., 2012. Electrochemical treatment of distillery spent wash using aluminum and iron electrodes. *Chinese Journal of Chemical Engineering*, 20(3), pp. 439-443.

Khor, C.P., Jaafar, M.B. and Ramakrishnan, S., 2016. Optimization of conductive thin film epoxy composites properties using desirability optimization methodology. *Journal of Optimization*, 2016, pp. 1-8.

Kommineni, S., Zoeckler, J., Stocking, A., Liang, S., Flores, A. and Kavanaugh, M., 2008. Advanced oxidation process. pp. 111-208.

Kuśmierek, K., Świątkowski, A. and Dąbek, L., 2015. Oxidative degradation of 2-chlorophenol by persulphate. *Journal of Ecological Engineering*, 16(3), pp. 115-123.

Lekhlif, B., Oudrhiri, L., Zidane, F., Drogui, P. and Blais, J.F., 2014. Study of the electrocoagulation of electroplating industry wastewaters charged by nickel (II) and chromium (VI). *J. Mater. Environ. Sci.*, 5(1), pp. 111-120.

Liew, W.L., Loh, S.K., Kassim, M.A. and Muda, K., 2015. Efficiency of nutrients removal from palm oil mill effluent treatment systems. *Journal of Oil Palm Research*, 27(4), pp. 433-443.

Ling, L.Y., 2007. *Treatability of palm oil mill effluent (POME) using black liquor in an anaerobic treatment process*. Postgraduate. Universiti Sains Malaysia.

Lorestani, A.A.Z., 2006. *Biological treatment of palm oil mill effluent (POME) using an up-flow anaerobic sludge fixed film (UASFF) bioreactor*. PhD. Universiti Sains Malaysia.

Madaki, Y.S. and L, Seng., 2013. Palm Oil Mill Effluent (POME) from Malaysia palm oil mills: waste or resource. *International Journal of Science, Environment and Technology*, 2(6), pp. 1138-1155.

Mahat, S.B.A., 2012. *The palm oil industry from the perspective of sustainable development: a case study of Malaysian palm oil industry*. Postgraduate. Ritsumeikan Asia Pacific University Japan.

Malaysian Palm Oil Board, 2008. *Monthly export of oil palm products - 2008 - January – December 2008*. [online] Available at: <http://bepi.mpob.gov.my/index.php/statistics/export/58-export-2008/201-monthly-export-of-oil-palm-products-2008.html> [Accessed 10 February 2015].

Malaysian Palm Oil Board, 2008. *Production of crude palm oil for month of December 2008 - January - December 2008.* [online] Available at: <http://bepi.mpob.gov.my/index.php/statistics/production/51-production-2008/166-production-of-crude-oil-palm-2008.html> [Accessed 5 February 2015].

Malaysian Palm Oil Board, 2011. *Malaysian Palm Oil Industry.* [online] Available at: <http://www.palmoilworld.org/about_malaysian-industry.html> [Accessed 5 February 2015].

Malaysian Palm Oil Board, 2011. *Malaysian Palm Oil Industry.* [online] Available at: <http://www.palmoilworld.org/about_malaysian-industry.html> [Accessed 5 February 2015].

Malaysian Palm Oil Board, 2014. *Oil Palm & The Environment.* [online] Available at: <http://www.mpob.gov.my/palm-info/environment/520-achievements> [Accessed 5 February 2015].

Malaysian Palm Oil Board, 2015. *Monthly export of oil palm products - 2015 - January – December 2015*. [online] Available at: <http://bepi.mpob.gov.my/index.php/statistics/export/138-export-2015/759-monthly-export-of-oil-palm-products-2015.html> [Accessed 10 February 2015].

Malaysian Palm Oil Board, 2015. *Production of crude palm oil for month of December 2015 - January - December 2015.* [online] Available at: <http://bepi.mpob.gov.my/index.php/statistics/production/135-production-2015/736-production-of-crude-oil-palm-2015.html> [Accessed 5 February 2015].

Malaysian Palm Oil Council, 2006. *Oil palm: tree of life*. 1st ed. Selangor: Malaysian Palm Oil Council.

Malaysian Palm Oil Council, 2007. *Malaysian Palm Oil.* [online] Available at: <http://www.meoa.org.my/phocadownloadpap/3.Marketing/Fact%20Sheet%20-%20Malaysian%20Palm%20Oil.pdf> [Accessed 5 February 2015].

Martínez-Huitle, C.A. and Andrade, L.S., 2011. Electrocatalysis in wastewater treatment: recent mechanism advances. *Quim. Nova*, 34(5), pp. 850-858.

Mickova, I., 2015. Advanced electrochemical technologies in wastewater treatment. Part II: electro-flocculation and electro-floatation. *American Scientific Research Journal for Engineering, Technology, and Sciences (ASRJETS)*, 14(2), pp. 273-294.

Miettinen, J., Hooijer, A., Tollenaar, D., Page, S., Malins, C., Vernimmen, R., Shi, C.H. and Liew, S.C., 2012. Historical analysis and projection of oil palm plantation expansion on Peatland in Southeast Asia. *The International Council on Clean Transportation*, pp. 3-51.

Mohajeri, S., Aziz, H.A., Isa, M.H., Zahed, M.A., Bashir, M.J.K. and Adlan, M.N., 2010. Application of the central composite design for condition optimization for semi-aerobic landfill leachate treatment using electrochemical oxidation. *Water Sci Technol*, 61(5), pp. 1257-1266.

Mohammed, R.R. and Chong, M.F., 2014. Treatment and decolorization of biologically treated palm oil mill effluent (POME) using banana peel as novel biosorbent. *Journal of Environmental Management*, 132(2014), pp. 237-249.

Moreno, H.A., Cocke, D.L., Gomes, J.J.A., Morkovsky, P., Parga, J.R. and Peterson, E., 2007. Electrocoagulation mechanism for COD removal. *Separation and Purification Technology*, 56 (2), pp. 204-211.

Morsi, M.S., Al-Sarawyb, A.A. and El-Deinb, W.A.S., 2011. Electrochemical degradation of some organic dyes by electrochemical oxidation on a Pb/PbO_2 electrode. *Desalination and Water Treatment*, 26(1-3), pp. 301-308.

Mutamin, N.S.A., Noor, Z.Z., Hassan, M.A.A., Yuniarto, A. and Olsson, G., 2013. Membrane bioreactor: applications and limitations in treating high strength industrial wastewater. *Chemical Engineering Journal*, 225 (2013), pp. 109-119.

Myers, R. H., Montgomery, D.C. & Anderson-Cook, C.M., 2009. *Response surface methodology, process and product optimization using designed experiments*. 3rd ed. Hoboken: John Wiley and Sons, Inc.

Naddeo, V., Cesaro, A., Mantzavinos, D., Fatta-Kassinos, D. and Belgiorno, V., 2014. Water and wastewater disinfection by ultrasound irradiation – a critical review. *Global NEST Journal*, 16(3), pp. 561-577.

Nagi, J., Ahmed, S.K. and Nagi, F., 2008. Palm biodiesel an alternative green renewable energy for the energy demands of the future. *International Conference on Construction and Building Technology*, 7, pp. 79-94.

Naje, A.S., Chelliapan, S., Zakaria, Z. and Abbas, S.A., 2015. Enhancement of an electrocoagulation process for the treatment of textile wastewater under combined electrical connections using titanium plates. *Int. J. Electrochem. Sci.*, 10(6), pp. 4495-4512.

Nasrullah, M., Singh, L. and Wahid, Z.A., 2012. Treatment of sewage by electrocoagulation and the effect of high current density. *Energy and Environmental Engineering Journal*, 1(1), pp. 27-31.

Nasseri, S., Vaezi, F., Mahvi, A.H., Nabizadeh, R. and Haddadi, S., 2006. Determination of the ultrasonic effectiveness in advanced wastewater treatment. *Iran. J. Environ. Health. Sci. Eng*, 3(2), pp. 109-116.

Ni'am, M.F., Othman, F., Sohaili, J. and Fauzia, Z., 2007. Electrocoagulation technique in enhancing COD and suspended solids removal to improve wastewater quality. *Water Science & Technology*, 56(7), pp. 47-53.

Ocampo, A.M., 2009. *Persulphate activation by organic compounds*. PhD. Washington State University.

Ozyonar, F. and Karagozoglu, B., 2012. Systematic assessment of electrocoagulation for the treatment of marble processing wastewater. *Int. J. Environ. Sci. Technol.*, 9(4), pp. 637-646.

Padmanabhan, A.R., 2008. *Novel simultaneous reduction/oxidation process for destroying organic solvents*. Postgraduate. Worcester Polytechnic Institute.

Quiroz, M.A., Bandala, E.R. and Martínez-Huitle, C.A., 2011. Advanced oxidation processes (AOPs) for removal of pesticides from aqueous media. In: M. Stoytcheva, ed. *Pesticides - formulations, effects, fate*. Croatia: Intech, pp. 686-730.

Rahmalan, M.T.B., 2009. *Electrocoagulation for suspended solid removal in domestic wastewater treatment*. Postgraduate. Universiti Teknologi Malaysia.

Ravindra, P., 2015. *Advances in bioprocess technology*. 1st ed. Switzerland: Springer International Publishing.

Rupani, P.F., Singh, R.P., Ibrahim, M.H. and Esa, N., 2010. Review of current palm oil mill effluent (POME) treatment methods: vermicomposting as a sustainable practice. *World Applied Sciences Journal*, 11(1), pp. 70-81.

Saberi, N.I.B., 2010. *Degradation of phenol by ultrasonic irradiation in addition of salt*. Undergraduate. Universiti Malaysia Pahang.

Salihu, A. and Alam, M.Z., 2012. Palm oil mill effluent: a waste or a raw material. *Journal of Applied Sciences Research*, 8(1), pp. 466-473.

Segneanu, A.E., Orbeci, C., Lazau, C., Sfirloaga, P., Vlazan, P., Bandas, C. and Grozescu, I., 2013. Waste water treatment methods. In: W. Elshorbagy and R.K. Chowdhury, eds. *Water treatment*. Croatia: Intech. pp. 53-80.

Setia, A., Kansal, S. and Goyal, N., 2013. Development and optimization of enteric coated mucoadhesive microspheres of duloxetine hydrochloride using 3^2 full factorial design. *Int J Pharm Investig*, 3(3), pp. 141-150.

Shah, M., 2014. Effective treatment systems for azo dye degradation: a joint venture between physico-chemical & microbiological process. *International Journal of Environmental Bioremediation & Biodegradation*, 2(5), pp. 231-242.

Shahrifun, N.S.A., Ab'lah, N.N., Hussain, H., Aris, A., Omar, Q. and Ahmad, N., 2015. Characterization of palm oil mill secondary effluent (POMSE). *Malaysian Journal of Civil Engineering*, 27(1), pp. 144-151.

Shi, G.Y., 2015. *Oxidation of 2,4-D using iron activated persulfate and peroxymonosulfate*. Postgraduate. Iowa State University.

Sogaard, E., 2014. *Chemistry of advanced environmental purification processes of water: fundamentals and applications*. Netherlands: Elsevier.

Stasinakis, A.S., 2008. Use of selected advanced oxidation processes (AOPs) for wastewater treatment - a mini review. *Global NEST Journal*, 10(3), pp. 376-385.

Sun, H.Q. and Wang, S.B., 2015. Catalytic oxidation of organic pollutants in aqueous solution using sulfate radicals. In: J.J. Spivey, Y.F. Han and K.M. Dooley, eds. *Catalysis*. United Kingdom: The Royal Society of Chemistry. pp. 107-114.

Symczycha, B. and Pempkowiak, J., 2016. *The role of submarine groundwater discharge as material source to the Baltic sea*. Switzerland: Springer International Publishing.

Talinli, I. and Anderson, G.K., 1992. Interference of hydrogen peroxide on the standard COD test. *Wat. Res.*, 26(1), pp. 107-110.

Tham, M.H., 2015. *Electro oxidation of palm oil mill effluent (POME): post treatment*. Undergraduate. Universiti Tunku Abdul Rahman.

Ujang, Z., Salmiati. and Salim, M.R., 2010. Microbial biopolymerization production from palm oil mill effluent (POME). In: L. Porijo, ed. *Biopolymers*. Croatia: Sciyo. pp. 473-494.

Vigneswaran, S., 2008. *Water and wastewater treatment technologies*. 1st ed. Australia: Encyclopedia of Life Support Systems (EOLSS).

Wang, Y.H., Chen, Q.Y., Li, G. and Li, X.L., 2012. Anodic materials with high energy efficiency for electrochemical oxidation of toxic organics in waste water. In: S.K. Yeow and X.X Guo, eds. *Industrial waste*, Croatia: Intech, pp. 34-52.

Williams, R., 2015. *Review of multiple regression*. [online] Available at: < https://www3.nd.edu/~rwilliam/stats2/l02.pdf> [Accessed 28 July 2016].

Wilson, S., Farone, W., Leonard, G., Birnstingl, J. and Leombruni, A., 2013. Catalyzed persulfate: advancing in situ chemical oxidation (ISCO) technology. *Pollution Engineering*, 45(6), pp. 1-16.

Wong, Y.S., 2007. *Chemical oxygen demand (COD) reduction efficiency and kinetic evaluation of anaerobic digestion process of palm oil mill effluent (POME) in anaerobic bench scale reactor (ABSR)*. Postgraduate. Universiti Sains Malaysia.

Worch, E., 2012, *Adsorption technology in water treatment: fundamentals, processes, and modeling*. Germany: De Gruyter.
world market to 2035. *Renewable and Sustainable Energy Reviews*, 39(2014), pp. 740-747.

Zahrim, A.Y., 2014. Palm oil mill biogas producing process effluent treatment: a short review. *Journal of Applied Sciences*, 14(23), pp. 3149-3155.

Zheng, C.L., Zhao, L., Zhou, X.B., Fu, Z.M. and Li, A., 2013. Treatment technologies for organic wastewater. In: W. Elshorbagy and R.K. Chowdhury, eds. *Water treatment*. Croatia: Intech. pp. 250-286.

Zhu, X.M., Nguyen, N.L., Sun, B., Li, Z.R. and Zhan, P.H., 2014. Phenolic wastewater treatment by pulsed electrolysis with alternative current. In: A. Sheng, ed. *Energy, environment and green building materials*. London: Taylor & Francis Group. pp. 105-108.

APPENDICES

APPENDIX A: Tables of Preliminary Results

Table A1 Effect of $S_2O_8^{2-}$ on COD Removal

$S_2O_8^{2-}$ Dosage, g	COD Removal Efficiencies, %
0.7908	76.34
1.5815	78.05
3.9537	67.05

Table A2 Effect of $S_2O_8^{2-}$ on Colour Removal

$S_2O_8^{2-}$ Dosage, g	Colour Removal Efficiencies, %
0.7908	97.50
1.5815	97.73
3.9537	97.99

APPENDIX B: ANOVA Results

Response 1 COD

ANOVA for Response Surface Reduced Quadratic Model

Analysis of variance table [Partial sum of squares - Type III]

Source	Sum of Squares	df	Mean Square	F Value	p-value Prob > F	
Model	1135.30	9	126.14	185.24	< 0.0001	significant
A-Current De	*70.62*	*1*	*70.62*	*103.70*	*< 0.0001*	
B-Contact Tir	*564.67*	*1*	*564.67*	*829.22*	*< 0.0001*	
C-Initial pH	*13.87*	*1*	*13.87*	*20.37*	*0.0002*	
D-Persulphat	*218.55*	*1*	*218.55*	*320.93*	*< 0.0001*	
AB	*14.57*	*1*	*14.57*	*21.40*	*0.0002*	
AD	*9.23*	*1*	*9.23*	*13.55*	*0.0015*	
BD	*26.19*	*1*	*26.19*	*38.46*	*< 0.0001*	
B^2	*2.97*	*1*	*2.97*	*4.35*	*0.0499*	
D^2	*1.11*	*1*	*1.11*	*1.63*	*0.2157*	
Residual	13.62	20	0.68			
Lack of Fit	*13.34*	*15*	*0.89*	*15.91*	*0.0032*	*significant*
Pure Error	*0.28*	*5*	*0.056*			
Cor Total	1148.92	29				

Figure B1 ANOVA of COD Removal

Response 2 Colour

ANOVA for Response Surface Reduced Quadratic Model

Analysis of variance table [Partial sum of squares - Type III]

Source	Sum of Squares	df	Mean Square	F Value	p-value Prob > F	
Model	5580.23	8	697.53	65.02	< 0.0001	significant
A-Current De	*124.23*	*1*	*124.23*	*11.58*	*0.0027*	
B-Contact Tir	*3342.56*	*1*	*3342.56*	*311.58*	*< 0.0001*	
C-Initial pH	*79.97*	*1*	*79.97*	*7.45*	*0.0125*	
D-Persulphat	*89.74*	*1*	*89.74*	*8.37*	*0.0087*	
AB	*118.92*	*1*	*118.92*	*11.09*	*0.0032*	
BC	*92.54*	*1*	*92.54*	*8.63*	*0.0079*	
BD	*91.01*	*1*	*91.01*	*8.48*	*0.0083*	
B^2	*1641.26*	*1*	*1641.26*	*152.99*	*< 0.0001*	
Residual	225.29	21	10.73			
Lack of Fit	*225.03*	*16*	*14.06*	*277.15*	*< 0.0001*	*significant*
Pure Error	*0.25*	*5*	*0.051*			
Cor Total	5805.52	29				

Figure B2 ANOVA of Colour Removal

Response 3 Suspended Solids

ANOVA for Response Surface Reduced Quadratic Model

Analysis of variance table [Partial sum of squares - Type III]

Source	Sum of Squares	df	Mean Square	F Value	p-value Prob > F	
Model	4070.97	8	508.87	61.29	< 0.0001	significant
A-Current De	*135.59*	*1*	*135.59*	*16.33*	*0.0006*	
B-Contact Tir	*2351.46*	*1*	*2351.46*	*283.21*	*< 0.0001*	
C-Initial pH	*82.12*	*1*	*82.12*	*9.89*	*0.0049*	
D-Persulphat	*85.84*	*1*	*85.84*	*10.34*	*0.0042*	
AB	*129.56*	*1*	*129.56*	*15.60*	*0.0007*	
BC	*82.86*	*1*	*82.86*	*9.98*	*0.0047*	
BD	*78.72*	*1*	*78.72*	*9.48*	*0.0057*	
B^2	*1124.81*	*1*	*1124.81*	*135.47*	*< 0.0001*	
Residual	174.36	21	8.30			
Lack of Fit	*174.27*	*16*	*10.89*	*616.53*	*< 0.0001*	*significant*
Pure Error	*0.088*	*5*	*0.018*			
Cor Total	4245.33	29				

Figure B3 ANOVA of SS Removal